OPEN ACCESS
Freely Available Online

Journal of New Developments in Chemistry
ISSN NO: 2377-2549

Research Article

DOI : 10.14302/issn.2377-2549.jndc-16-1119

Vibrational, Ultra Violet, Natural Bond Orbital analysis of E-[1-(3'-methylthienyl)-5-Phenyl-2, 4-Pentadiene-3-one] using Quantum Mechanical Computations and Experimental Spectra.

D.Sumathi[1], H. Saleem[1]*, S.Srinivasan[2], N.RameshBabu[3],D.Usha[4]

1. Department of Physics, Annamalai University, Annamalainagar-608 002, Tamil Nadu, India
2. Department of Chemistry, Annamalai University, Annamalainagar-608 002, Tamil Nadu, India
3. Department of Physics, MIET Engineering College, Tiruchirappalli – 620 007, Tamil Nadu, India
4. Department of Physics, Women's Christian college, Nagercoil – 629 001, Tamil Nadu, India

ABSTRACT

The FT-IR, FT-Raman and UV-Vis spectra of E-[1-(3'-methylthienyl)-5-Phenyl-2,4-Pentadiene-3-one (MPPO) were recorded. The optimized molecular bond parameters, harmonic frequencies were calculated using B3LYP method with 6-311++G (d,p) basis set.The various normal modes were precisely assigned with thehelp ofTED calculation. The theoretical spectrograms for FT-IR, FT-Raman and Ultra Violet visible. Spectra of the title molecule had been constructed. The ICT was calculated by means of Natural Bond Orbital analysis. The Non Linear Optical properties related to polarizability and hyperpolarizability based on the finite-field approach were calculated.The band gap energy was calculated using HOMO-LUMO analysis. Furthermore, the Molecular Electrostatic Potential, Mulliken atomic charges and thermodynamic properties of MPPO were also calculated.

Corresponding author: H. Saleem, Department of Physics, Annamalai University, Annamalainagar-608 002, Tamil Nadu, India, saleem_h2001@yahoo.com.

Citation: D.Sumathi , H. Saleem, S.Srinivasan , N.RameshBabu , D.Usha (2016) Vibrational, Ultra Violet, Natural Bond Orbital Analysis of E-1 using Quantum Mechanical Computations and Experimental Spectra.. Journal Of New Developments In Chemistry - 1(2):26-57. https://doi.org/10.14302/issn.2377-2549.jndc-16-1119

Keywords: MPPO, DFT, NLO, NBO, MEP

Received May 21, 2016; **Accepted** Aug 04, 2016; **Published** Sep 06, 2016;

Academic Editor: Dr. Praveen Kumar Sharma, Lovely Professional University, Phagwara, Punjab, India-144411

Introduction

Chalcones belong to the flavonoid families which are synthesized in factories to preserve the health of plants against infections and parasites. They have attractedincreasing attention due to numerous pharmacological applications [1-8].It possess various multipronged activities such as anti-microbial [9], anti-depressants [10], anti-plasmodial [11], anti-aids [12], insect anti-feedant activities [13 &14], biological treatment due to its good anti-malaria [15], and in vitro anti-tumor activity [16]. It exhibits radical quenching and hydroxyl adducts formation [17]. Whilst chalcones are active against various protein targets, modification of the privileged core could lead to novel compounds with specifically targeted inhibitory activity [18].

Chidan Kumar et al., [19] synthesized the high quality single crystal of efficient novel NLO chalcone derivative (2E)-1-(5-chlorothiophen-2-yl)-3-(2,3,4-trimethoxyphenyl) prop-2-en-1-one and its structure was characterized by FTIR, FT-Raman and single crystal XRD techniques. The vibrational wavenumbers were computed using DFT and were assigned on the basis of PED analysis. The geometrical parameters obtained from XRD studywere compared with the calculated values by applying DFT/6-31G (d,p) basis set. Stability of the molecule, hyper conjugative interactions, charge delocalization and intra-molecular hydrogen bond had been studied using NBO analysis. Karunakaran et al., [20] reported the FTIR and FT-Raman spectra of trans-3 -(o-hydroxyphenyl-1-phenyl)-2-propen-1-one (or simply 2-hydroxychalcone) were recorded in the regions 4000–400 cm^{-1} and 3500–100 cm^{-1}, respectively in the solid phase. The vibrational wavenumbers were calculated by HF and DFT/B3LYP methods with 6-311++G (d, p) basis set, using Gaussian 09W program package. A detailed interpretation of the IR and Raman spectra of 2-hydroxychalcone was reported.

In light of the above literature survey, it was clear that inspite of many important applications of MPPO not many works were carried out on this molecule; particularly the complete vibrational analysis supported by quantum computations was not carried out. Hence in this study, FTIR, FT-Raman and UV-Vis. spectral analysis of the compound MPPO was carried out. The NBO analysis, with emphasis on HOMO-LUMO, NLO, MEP, Mulliken's charges, and various thermodynamic parameters were also calculated using quantum computations by DFT/B3LYP method.

Experimental Details

Synthesis Procedure

Mono benzal acetone (1.46g, 0.01mol) was dissolved in 15 mL of ethanol with slight warning. To this hot solution methyl thiophen-2-carboxaldehyde (1.4 mL, 0.01mol) and few drops of solution hydroxide solution 10%) were added. The solution gradually turned red on warming and yellow crystals separated. The product was filtered off and recrystalised twice from ethanol. The yield and melting point of the crystal is 76% and 148 respectively.

Instrumentation

FT-IR, FT-Raman and UV–Vis spectra

The FT-IR spectrum on an IFS 66v spectrophotometer of MPPO was recorded in the spectral region between 400–4000 cm^{-1} using the KBr pellet technique. The spectrum was recorded at room temperature with a scanning speed of 10 cm^{-1} per minute and at the spectral resolution of 2.0 cm^{-1} in the

Department of Chemistry, Jamal Mohamed College, Trichy, Tamilnadu, India. The FT-Raman spectrum of title compound was recorded using the 1064 nm line of an Nd: YAG laser as excitation wavelength in the region 50–3500 cm^{-1} on Bruker model IFS 66V spectrophotometer equipped with an FRA 106 FT-Raman module accessory and at spectral resolution of 4 cm^{-1}. The FT-Raman spectral measurement was carried out from SAIF Laboratory, IIT Madras, Tamilnadu, India. The UV-Vis absorption spectrum of MPPO was recorded in the range of 200–500 nm using a Shimadzu – 2600 spectrometer in the Department of Chemistry, Jamal Mohamed College, Trichy-20. The UV pattern was taken from a 10^{-5} molar solution of MPPO dissolved in benzene.

Computational Details

For meeting the requirements of both accuracy and computing economy, theoretical methods and basis sets should be considered. DFT had proved to be extremely useful in treating electronic structure of molecules. The density functional theory parameter hybrid model [DFT/B3LYP/6-311++G(d,p)] basis set was adopted to calculate the properties of the title molecule in this work[50] . All the calculations were performed using the Gaussian 03W program package [21] with the default convergence criteria without any constraint on the geometry [22]. It should be noted that Gaussian 03W package did not calculate the Raman intensities. The Raman activities were transformed into Raman intensities using Raint program [23].

Results and Discussion

Molecular Geometry

The optimized geometrical parameters for MPPO are calculated using B3LYP/6-311++G(d,p) level of calculation and are presented in Table.1 in accordance with atom numbering given in Fig.1. The title molecule consists of thiophene and phenyl ring fused by carbonyl group. In MPPO the C=O group plays an important role. The carbonyl (C_{16}=O_{17}) bond length is observed at 1.190 Å[24], whereas the calculated bond length is about 1.235Å.In thiophen ring, the two C-S bond lengths are found at 1.707 and 1.728Å.In this study, the C_1-S_5 (1.762Å) and C_4-S_5(1.717Å) bond lengths are differ by 0.045Å and the bond angles C_2-C_1-S_5(110.34°) and C_3-C_4 -S_5(112.86°) also differ by 2.52°,which is due to the shortening of bond distance between atoms C_1 and S_5 atoms. The bond angle O_{17}-C_{16}-C_{18}(124.37°) is positively (~2.98°) from C_{14}-C_{16}-O_{17}(121.39°). This may be due the intra- or inter-molecular interaction S---O---H. From the theoretical values, it is found that most of the optimized bond parameters are slightly greater than the experimental values, since the calculation has been done on a single molecule in gaseous state.Although the differences, calculated geometrical parameters represent a good approximation and they can be used as foundation to calculate the other parameters, such as vibrational frequencies and thermodynamics properties.The calculated bond parameters are compared with experimental values[24, 25]. The

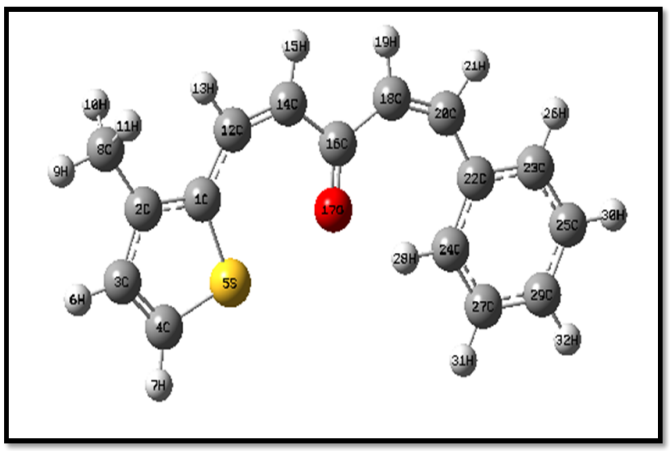

Fig. 1. The optimized molecular structure of MPPO

optimized structure is planar as it is evident from the dihedral angles $C_{12}C_{14}C_{16}O_{17}$=0.00° & $C_{12}C_{14}C_{16}C_{18}$=-180.00°; $C_{14}C_{16}C_{18}C_{20}$=180.00° & $O_{17}C_{16}C_{18}C_{20}$=-0.00°;$C_2C_1C_{12}C_{14}$=179.99°& $S_5C_1C_{12}C_{14}$=-0.00° and $C_{18}C_{20}C_{22}C_{23}$=-179. 99° & $C_{18}C_{20}C_{22}C_{24}$=0.00° are listed in Table.1.

Vibrational Assignments

The molecule MPPO belongs to C_1 point group symmetry. This molecule has 32 atoms and hence90 normal modes of fundamental vibrations are possible, which span the irreducible representation:61A'+29A". All the 90 fundamental modes are active in both IR and Raman. The vibrational analysis of MPPO is performed on the basis of the characteristic vibrations of carbonyl, methyl, thiophene, pentadiene and phenyl ring modes. In this study, the harmonic vibrational frequencies are calculated at B3LYP level using 6-311++G(d,p)basis set have been collected in Table2. Some discrepancies could be identified in between harmonic and experimental frequencies, which are scaled down by proper scale factor [26]. To find the exact vibrational behavior of this molecule the TED analysis was performed on the gas phase. The combined experimental and theoretical spectra are shown in Figs.2 and 3.

C=O Vibrations

The carbonyl stretching frequency has been most extensively studied by IR spectroscopy [27]. The multiply bonded group is highly polar and therefore gives rise to an intense IR absorption band. The carbon–oxygen double bond is formed by Pπ–Pπ bonding between carbon and oxygen atoms. The loan pair of electrons on oxygen also determines the nature the carbonyl group. The vC=O mode of carboxylic acids is identical to the vC=O mode in ketones, which is expected in the region 1660-1740 cm^{-1}[28].The stretching vibration of carbonyl group C=O can be observed as a very strong band in both FTIR and FT-Raman spectra at 1665cm^{-1}[29,30].According to above literature strong band observed in FTIR spectrum at 1647 cm^{-1} and weak band in FT-Raman spectrum at 1647 cm^{-1} is assigned to C=O stretching vibration.The value of this band is calculated 1629cm^{-1} (mode no:15) with a TED of 85%. This assignment is in moderate agreement with literature [31] in the case of thiophene-2-carohydrazide. The observed very weak band in FT-Raman at 724cm^{-1} is ascribed to $\beta C_{16}=O_{17}$ mode, while its correspondingharmonic frequency is 733cm^{-1} (mode no:60). These assignments are also supported by the literature[31]in addition to TED (36%) output.

C-S Vibrations

The C-S stretching vibration is well known to mix with neighboring modes [32].Literature survey revealed that v(C-S) vibration of thiophene ring was observed in the region 719-842cm^{-1}[33]. The harmonic wave numbers 811,687 (mode nos:56,63) and FTIR band observed at 812 cm^{-1} are assigned to ν_{C-S} modes. These modes are mixed with β_{CCC} modes and also have considerable TED (>32%) values. Furthermore, these assignments also find support from the literature[34].

Methyl Group Vibrations

Methyl groups are generally referred to as electron donating substituents in the aliphatic and aromatic ring system [35]. For the assignments of CH_3 group, basically nine fundamentals can be associated with each CH_3 group namely: the symmetrical stretching in CH_3 (CH_3sym. stretching); anti-symmetrical stretching

Table 1. The optimized bond parameters of MPPO using B3LYP/6-311++G(d,p) basis set

Parameters	B3LYP/ 6-311++G(d,p)	XRD [a,b,c,d]
Bond Lengths (Å)		
C1-C2	1.401	1.375[a], 1.362[b]
C1-S5	1.762	1.728[b]
C1-C12	1.436	
C2-C3	1.415	1.431[a], 1.392[b]
C2-C8	1.507	
C3-C4	1.372	1.37[d], 1.345[b]
C3-H6	1.083	1.081[c]
C4-S5	1.717	1.717[a], 1.707[b], 1.714[d]
C4-C7	1.081	
C8-H9	1.091	
C8-H10	1.094	
C8-H11	1.094	
C12-H13	1.087	0.950 (6)[c]
C12-C14	1.361	
C14-H15	1.085	0.951 (8)[c]
C14-C16	1.467	
C16-C18	1.479	
C16-O17	1.235	1.190 (3)[c]
C18-H19	1.086	0.951 (8)[c]
C18-C20	1.358	
C20-H21	1.089	0.950 (6)[c]
C20-C22	1.463	
C22-C23	1.412	1.366 (4)[c]
C22-C24	1.409	
C23-C25	1.389	
C23-H26	1.085	0.954 (2)[c]
C24-C27	1.391	
C24-H28	1.08	0.949 (2)[c]
C25-C29	1.395	
C25-H30	1.084	0.950 (3)[c]
C27-C29	1.395	
C27-H31	1.084	0.950 (2)[c]
C29-H32	1.085	0.950 (3)[c]

Parameters	B3LYP/ 6-311++G(d,p)	XRD [a,b,c,d]
Bond Angles (°)		
C2-C1-S5	110.34	111.80[a]
C2-C1-C12	122.15	
S5-C1-C12	127.51	
C1-C2-C3	112.64	112.20[a], 114.72[b], 112.5[d]
C1-C2-C8	124.93	
C3-C2-C8	122.43	
C2-C3-C4	112.9	112.05[b]
C2-C3-H6	123.42	123.3[d]
C4-C3-H6	123.68	
C3-C4-S5	112.86	112.13[b]
C3-C4-H7	127.42	
S5-C4-H7	119.72	
C1-S5-C4	91.27	92.00[a], 91.81[b], 92.2[d]
C2-C8-H9	110.2	
C2-C8-H10	111.96	
C2-C8-H11	111.96	
H9-C8-H10	107.48	
H9-C8-H11	107.48	
H10-C8-H11	107.55	
C1-C12-H13	110.92	
C1-C12-C14	135.87	
H13-C12-C14	113.2	121.2 (6)[c]
C12-C14-H15	115.61	116.1 (7)[c]
C12-C14-C16	128.31	127.7 (6)[c]
H15-C14-C16	116.08	116.3 (6)[c]
C14-C16-O17	121.39	106.5 (3)[c]
C14-C16-C18	114.24	147.1 (4)[c]
O17-C16-C18	124.37	106.5 (3)[c]
C16-C18-H19	113.14	116.3 (6)[c]
C16-C18-C20	132.74	127.7 (6)[c]
H19-C18-C20	114.12	116.1 (7)[c]
C18-C20-H21	112.56	121.2 (6)[c]
C18-C20-C22	136.42	117.6 (5)[c]
H21-C20-C22	111.03	121.2 (4)[c]
C20-C22-C23	116.08	140.3 (3)[c]
C20-C22-C24	125.99	101.8 (3)[c]
C23-C22-C24	117.93	117.5 (2)[c]
C22-C23-C25	121.5	121.2 (3)[c]
C22-C23-H26	119.09	119.4 (3)[c]
C25-C23-H26	119.41	119.4 (3)[c]
C22-C24-C27	120.34	120.4 (2)[c]
C22-C24-H28	118.84	119.8 (2)[c]
C27-C24-H28	120.82	119.7 (2)[c]

Parameters	B3LYP/ 6-311++G(d,p)	XRD [a,b,c,d]
C23-C25-C29	119.76	120.4 (3)[c]
C23-C25-H30	119.96	119.8 (3)[c]
C29-C25-H30	120.29	119.8 (3)[c]
C24-C27-C29	120.88	120.8 (2)[c]
C24-C27-H31	119.27	119.6 (3)[c]
C29-C27-H31	119.85	119.6 (3)[c]
C25-C29-C27	119.59	119.7 (3)[c]
C25-C29-H32	120.15	120.2 (3)[c]
C27-C29-H32	120.26	120.2 (3)[c]
Dihedral Angles (°)		
S5-C1-C2-C3	0	
S5-C1-C2-C8	180	
C12-C1-C2-C3	180	
C12-C1-C2-C8	0	
C2-C1-S5-C4	0	
C12-C1-S5-C4	-180	
C2-C1-C12-H13	0	
C2-C1-C12-C14	179.99	
S5-C1-C12-H13	179.99	
S5-C1-C12-C14	0	
C1-C2-C3-C4	0	
C1-C2-C3-H6	180	
C8-C2-C3-C4	-179.99	
C8-C2-C3-H6	0	
C1-C2-C8-H9	-180	
C1-C2-C8-H10	60.43	
C1-C2-C8-H11	-60.44	
C3-C2-C8-H9	0	
C3-C2-C8-H10	-119.57	
C3-C2-C8-H11	119.56	
C2-C3-C4-S5	0	
C2-C3-C4-O7	-180	
H6-C3-C4-S5	-180	
H6-C3-C4-H7	0	
C3-C4-S5-C1	0	
H7-C4-S5-C1	180	
C1-C12-C14-H15	179.99	
C1-C12-C14-C16	0	
H13-C12-C14-H15	0	
H13-C12-C14-C16	179.99	
C12-C14-C16-O17	0	
C12-C14-C16-C18	-180	
H15-C14-C16-O17	180	
H15-C14-C16-C18	0	
C14-C16-C18-H19	0	

Parameters	B3LYP/ 6-311++G(d,p)	XRD [a,b,c,d]
C14-C16-C18-C20	180	
O17-C16-C18-H19	179.99	
O17-C16-C18-C20	0	
C16-C18-C20-H21	180	
C16-C18-C20-C22	0	
H19-C18-C20-H21	0	
H19-C18-C20-C22	179.99	
C18-C20-C22-C23	-179.99	
C18-C20-C22-C24	0	
H21-C20-C22-C23	0	
H21-C20-C22-C24	-179.99	
C20-C22-C23-C25	180	
C20-C22-C23-H26	0	
C24-C22-C23-C25	0	
C24-C22-C23-H26	180	
C20-C22-C24-C27	-180	
C20-C22-C24-H28	0	
C23-C22-C24-C27	0	
C23-C22-C24-H28	-180	
C22-C23-C25-C29	0	
C22-C23-C25-H30	-180	
H26-C23-C25-C29	180	
H26-C23-C25-H30	0	
C22-C24-C27-C29	0	
C22-C24-C27-H31	180	
H28-C24-C27-C29	180	
H28-C24-C27-H31	0	
C23-C25-C29-C27	0	
C23-C25-C29-H32	-180	
H30-C25-C29-C27	180	
H30-C25-C29-H32	0	
C24-C27-C29-C25	0	
C24-C27-C29-H32	180	
H31-C27-C29-C25	180	
H31-C27-C29-H32	0	

a O. Brathen, K. Kveseth, K.J. Nielsen, K. Hagen, J. Mol. Struct. 145 (1986) 45

b O.K. Geiger, H.C. Geiger, L. Williams, B.C. Noll, ActaCryst E68 (2012) o420

cVanchinathan et al., Physica B, 406 (2011) 4195

d Karol Pasterny et al., J. Mol. Struct, 614 (2002) 297-304

Table 2. The experimental and calculated frequencies of MPPO using B3LYP/6-311++G(d,p) level of basis set [harmonic frequencies (cm^{-1}), IR, Raman intensities (Km/mol), reduced masses (amu) and force constants ($mdynA°^{-1}$)]

Mode No	Calculated Frequencies (cm^{-1})		Observed Frequencies (cm^{-1})		IR Intensity	Raman Intensity	Reduced Masses	Force Consts	Vibrational Assignments≥10% (TED)[d]
	Un Scaled	Scaled[a]	FT-IR	FT-Raman	Rel.[b]	Rel.[c]			
1	3231	3104			0.03	0.61	1.1	6.75	$\nu C_{24}H_{28}(95)$
2	3225	3098			12.04	0.37	1.09	6.7	$\nu C_{14}H_{15}(98)$
3	3193	3068			2.69	0.6	1.09	6.55	$\nu C_{8}H_{11}(94)$
4	3188	3063	3064 vw	3059 vw	4.7	1.04	1.1	6.57	$\nu C_{8}H_{9}(83)$
5	3177	3052			4.94	0.33	1.09	6.5	$\nu C_{8}H_{10}(85)$
6	3172	3047			4.12	0.59	1.09	6.46	$\nu C_{18}H_{19}(87)$
7	3165	3041			0.42	0.38	1.09	6.42	$\nu C_{23}H_{26}(84)$
8	3158	3034			0.99	0.13	1.09	6.38	$\nu C_{12}H_{13}(72)$
9	3151	3027	3021 vw		0.77	0.08	1.09	6.37	$\nu C_{3}H_{6}(75)$
10	3139	3016			0.87	0.15	1.08	6.29	$\nu C_{20}H_{21}(83)$
11	3111	2989			1.45	0.17	1.08	6.19	$\nu C_{4}H_{7}(85)$
12	3106	2984			3.59	0.28	1.1	6.25	$\nu C_{25}H_{30}(92)$
13	3073	2953	2919 w	2921 vw	2.57	0.27	1.1	6.13	$\nu C_{27}H_{31}(100)$
14	3025	2907	2843 vw		6.13	1.12	1.04	5.6	$\nu C_{29}H_{32}(92)$
15	1696	1629	1647 s	1647 vw	12.94	3.2	7.03	11.91	$\nu C_{16}O_{17}(85)$
16	1642	1578	1617 m	1616 w	17.67	1.55	5.53	8.78	$\nu C_{24}C_{27}(18)+\nu C_{23}C_{25}(25)+\nu C_{25}C_{29}(14)+\beta H_{26}C_{23}C_{25}(15)$
17	1624	1560	1586 vs	1584 vs	100	21.83	5.42	8.43	$\nu C_{4}C_{3}(32)+\nu C_{24}C_{27}(12)$
18	1604	1541	1550 m	1551 vw	98.37	3.24	5.33	8.08	$\nu C_{18}C_{20}(46)+\beta H_{32}C_{29}C_{27}(20)$
19	1583	1521			4.3	100	7.4	10.93	$\nu C_{16}O_{17}(66)$
20	1534	1474	1492 m	1494 vw	5.18	0.67	3.93	5.44	$\nu C_{16}C_{18}(45)$
21	1524	1464			1.92	3.21	2.16	2.95	$\nu C_{12}C_{14}(12)+\beta H_{15}C_{14}C_{16}(50)$
22	1504	1445	1447 w		2.05	1.15	1.19	1.58	$\beta H_{10}C_{8}H_{11}(60)+\beta H_{13}C_{12}C_{14}(10)$
23	1495	1437			5.7	7.89	2.04	2.69	$\beta H_{13}C_{12}C_{14}(42)$
24	1490	1432			1.67	0.22	1.04	1.36	$\beta H_{9}C_{8}H_{10}(78)+\tau H_{9}C_{8}C_{2}C_{3}(10)+\tau H_{10}C_{8}C_{2}C_{3}(10)$
25	1486	1428			2.28	3.84	1.72	2.24	$\beta H_{21}C_{20}C_{22}(60)$
26	1467	1409	1404 m	1406 vw	2.2	0.77	1.82	2.31	$\beta H_{19}C_{18}C_{20}(58)$
27	1426	1370			8.06	2.12	2.81	3.36	$\nu C_{2}C_{3}(24)+\nu C_{1}C_{2}(14)+\beta H_{6}C_{3}C_{4}(25)$

Mode No	Calculated Frequencies (cm^{-1})		Observed Frequencies (cm^{-1})		IR Intensity	Raman Intensity	Reduced Masses	Force Consts	Vibrational Assignments≥10% (TED)[d]
	Un Scaled	Scaled[a]	FT-IR	FT-Raman	Rel.[b]	Rel.[c]			
28	1412	1357			0.31	0.87	1.28	1.51	$\beta H_9C_8H_{10}(88)$
29	1384	1330	1334 m		13.7	9.15	2.76	3.12	$\nu C_{14}C_{16}(50)$
30	1381	1327			5.07	8	1.45	1.63	$\beta H_{21}C_{20}C_{22}(65)$
31	1360	1307		1314 w	0.1	4.73	2.13	2.32	$\nu C_{18}C_{20}(14)+\nu C_{23}C_{25}(18)+\beta H_{26}C_{23}C_{25}(40)$
32	1342	1289			20.27	7.27	1.38	1.46	$\beta H_{13}C_{12}C_{14}(58)$
33	1299	1248		1258 w	0.51	0.51	1.83	1.82	$\nu C_{22}C_{24}(34)+\beta H_{28}C_{24}C_{27}(20)$
34	1261	1212	1193 m		0.44	0.02	1.76	1.65	$\nu C_2C_8(15)+\beta H_6C_3C_4(52)$
35	1216	1168	1183 m	1185 w	3.88	0.24	1.25	1.09	$\beta H_{26}C_{23}C_{25}(55)$
36	1205	1158			0.63	4.87	2.34	2	$\nu C_{20}C_{22}(25)$
37	1195	1148			4.24	0.45	2.1	1.77	$\nu C_1C_2(14)+\nu C_2C_3(10)+\beta H_{13}C_{12}C_{14}(12)$
38	1184	1137			0.01	0.16	1.11	0.92	$\beta H_{32}C_{29}C_{27}(60)$
39	1119	1075	1090 w	1090 m	36.76	1.15	1.92	1.42	$\nu C_{18}C_{20}(12)+\nu C_{16}C_{18}(24)+\beta H_{19}C_{18}C_{20}(12)+\beta H_7C_4S_5(16)$
40	1110	1066			0.16	0.21	1.35	0.98	$\nu C_2C_3(10)+\beta H_7C_4S_5(50)$
41	1097	1054			50.3	0.07	2.95	2.09	$\nu C_{16}C_{18}(26)$
42	1052	1011	1012 m		0.45	1.12	2.32	1.51	$\nu C_{25}C_{29}(48)+\beta H_{26}C_{23}C_{25}(18)+\beta C_{23}C_{25}C_{29}(12)$
43	1051	1010			0.17	0.03	1.5	0.98	$\beta H_9C_8H_{11}(22)+\tau H_9C_8C_2C_3(34)+\tau H_{10}C_8C_2C_3(34)$
44	1039	998		1000 w	1.25	0.56	1.78	1.13	$\nu C_2C_8(10)+\beta H_9C_8H_{10}(14)+\tau H_9C_8C_2C_3(20)+\tau H_{10}C_8C_2C_3(20)$
45	1032	991	985 vw		0.27	0.01	1.31	0.82	$\tau H_{28}C_{24}C_{27}C_{29}(72)$
46	1019	979			0	0.16	1.28	0.79	$\tau H_{19}C_{18}C_{20}C_{22}(78)$
47	1015	976			0.42	5.13	6.19	3.76	$\nu C_{27}C_{29}(22)+\beta C_{24}C_{27}C_{29}(50)$
48	997	958			0.01	0.24	1.29	0.75	$\tau H_{13}C_{12}C_{14}C_{16}(80)$
49	994	955			0.09	0.02	1.32	0.77	$\tau H_{32}C_{29}C_{27}C_{24}(70)$
50	973	935			2.46	0.51	2.83	1.58	$\nu C_{12}C_{14}(20)$
51	953	916			1.09	0.01	1.4	0.75	$\tau H_{26}C_{23}C_{25}C_{29}(78)$
52	930	894			1.52	0.64	3.7	1.89	$\nu C_{12}C_{14}(15)+\beta C_{14}C_{16}C_{18}(22)$
53	897	862			0.44	0.02	1.28	0.61	$\tau H_6C_3C_4S_5(76)$
54	865	831		834 vw	1.65	0	1.37	0.6	$\tau H_{19}C_{18}C_{20}C_{22}(78)$
55	859	825			8.59	0.02	2.06	0.89	$\tau H_{19}C_{18}C_{20}C_{22}(22)+\tau C_1C_{12}C_{14}C_{16}(18)+\tau H_{13}C_{12}C_{14}C_{16}(20)+\tau H_{30}C_{25}C_{29}C_{27}(14)$
56	844	811	812 m		8.45	0.33	4.61	1.93	$\nu C_4S_5(42)+\beta C_1C_2C_3(15)$
57	830	797			2.64	0.21	5.16	2.09	$\nu C_4S_5(28)+\beta C_1C_2C_3(18)$
58	809	777	760 vw		2.51	0.04	1.97	0.76	$\tau H_{13}C_{12}C_{14}C_{16}(12)+\tau H_{30}C_{25}C_{29}C_{27}(40)+\tau C_{22}C_{24}C_{27}C_{29}(12)$
59	767	737			0	0.07	1.65	0.57	$\tau C_1C_{12}C_{14}C_{16}(26)+\tau H_{13}C_{12}C_{14}C_{16}(38)$
60	763	733		724 vw	0.55	2.08	5.71	1.96	$\nu C_{20}C_{22}(18)+\beta C_{18}C_{16}O_{17}(36)$
61	734	705			13.14	0.03	1.23	0.39	$\tau H_6C_3C_4S_5(75)$
62	718	689	697 w	691 vvw	2.72	0.02	1.34	0.41	$\tau H_{19}C_{18}C_{20}C_{22}(44)+\tau C_1C_{12}C_{14}C_{16}(14)+\tau H_{30}C_{25}C_{29}C_{27}(26)$

Mode No	Calculated Frequencies (cm^{-1})		Observed Frequencies (cm^{-1})		IR Intensity	Raman Intensity	Reduced Masses	Force Consts	Vibrational Assignments≥10% (TED)[d]
	Un Scaled	Scaled[a]	FT-IR	FT-Raman	Rel.[b]	Rel.[c]			
63	715	687			0.12	7.15	6.89	2.07	$\nu C_4S_5(32)+\beta C_1C_2C_3(22)+\beta C_2C_3C_4(12)$
64	697	670			3.56	0.03	2.52	0.72	$\tau H_{28}C_{24}C_{27}C_{29}(12)+\tau C_{22}C_{24}C_{27}C_{29}(48)$
65	663	637		634 vvw	0.04	0.55	6.25	1.62	$\nu C_{12}C_{14}(22)+\beta C_{23}C_{25}C_{29}(12)+\beta C_1C_2C_3(14)+\beta C_2C_3C_4(10)$
66	632	607			0.21	0.43	6.31	1.48	$\beta C_{18}C_{20}C_{22}(62)$
67	625	601			0.14	0.11	2.93	0.68	$\tau H_{13}C_{12}C_{14}C_{16}(12)+\Gamma C_8C_1C_3C_2(58)$
68	603	579			0.6	0.83	5.49	1.18	$\nu C_1C_2(35)+\beta C_2C_1C_{12}(20)$
69	549	528		531 vw	0.28	0.31	7.08	1.26	$\beta C_1C_2C_3(10)+\beta C_1C_{12}C_{14}(24)$
70	529	508			0.23	1.58	6.2	1.02	$\nu C_2C_8(15)+\beta C_1C_2C_3(50)$
71	526	505			0.08	0.42	3.06	0.5	$\Gamma C_{20}C_{23}C_{24}C_{22}(65)$
72	490	470	455 m		2.31	0.02	3.2	0.45	$\Gamma C_{20}C_{23}C_{24}C_{22}(60)$
73	463	445	424 w		6.62	0.49	6.05	0.76	$\beta C_{22}C_{24}C_{27}(10)+\beta C_1C_{12}C_{14}(30)$
74	423	407		402 vw	0.3	0.24	3.28	0.35	$\tau C_1C_2C_3C_4(44)+\tau C_{23}C_{25}C_{29}C_{27}(22)$
75	412	395			0.14	0.15	3.14	0.31	$\tau C_1C_2C_3C_4(20)+\tau C_{23}C_{25}C_{29}C_{27}(42)$
76	358	344			0.12	0.53	3.61	0.27	$\beta C_3C_2C_8(60)$
77	350	336			0.34	0.13	3.4	0.25	$\tau C_{16}C_{18}C_{20}C_{22}(55)$
78	268	258			1.22	0.28	8.91	0.38	$\beta C_{14}C_{16}C_{18}(60)$
79	237	228			0.5	0.07	3.64	0.12	$\Gamma C_8C_1C_3C_2(62)+\Gamma C_{20}C_{23}C_{24}C_{22}(15)$
80	226	217			0.31	5.93	7.6	0.23	$\beta C_{18}C_{20}C_{22}(55)$
81	194	187			0.25	0.45	4.55	0.1	$\nu C_3C_4(12)+\beta C_2C_1C_{12}(40)$
82	180	173		164 vw	0.19	0.43	3.83	0.07	$\tau C_{24}C_{27}C_{29}C_{25}(55)+\Gamma C_{20}C_{23}C_{24}C_{22}(12)$
83	153	147			0.21	0.14	4.72	0.07	$\Gamma C_8C_1C_3C_2(14)+\Gamma C_{20}C_{23}C_{24}C_{22}(60)$
84	145	139			0.27	0.42	5.54	0.07	$\beta C_{22}C_{24}C_{27}(10)+\beta C_{24}C_{27}C_{29}$ (65)
85	110	106			0.02	0.27	1.03	0.01	$\tau H_9C_8C_2C_3(95)$
86	78	75		69 w	0.71	0.1	7.08	0.03	$\Gamma C_{20}C_{23}C_{24}C_{22}(75)$
87	52	50			0.03	5.81	6.66	0.01	$\beta C_{12}C_{14}C_{16}(78)$
88	47	45			0.02	3.67	4.51	0.01	$\tau C_2C_1C_{12}C_{14}(72)$
89	28	27			0.01	1.93	4.08	0	$\tau C_3C_2C_1C_{12}(62)$
90	14	13			0.22	0.06	5.21	0	$\tau C_1C_{12}C_{14}C_{16}(80)$

n: Stretching, β: in-plane-bending, Γ: out-of-plane bending, τ- Torsion, vw: very week, w: week, m: medium, s: strong, vs: very strong,

a Scaling factor: 0.9608,

bRelative IR absorption intensities normalized with highest peak absorption equal to 100,

c Relative Raman intensities calculated by Equation (1) and normalized to 100.

dTotal energy distribution calculated at B3LYP/6-311++G(d,p) level.

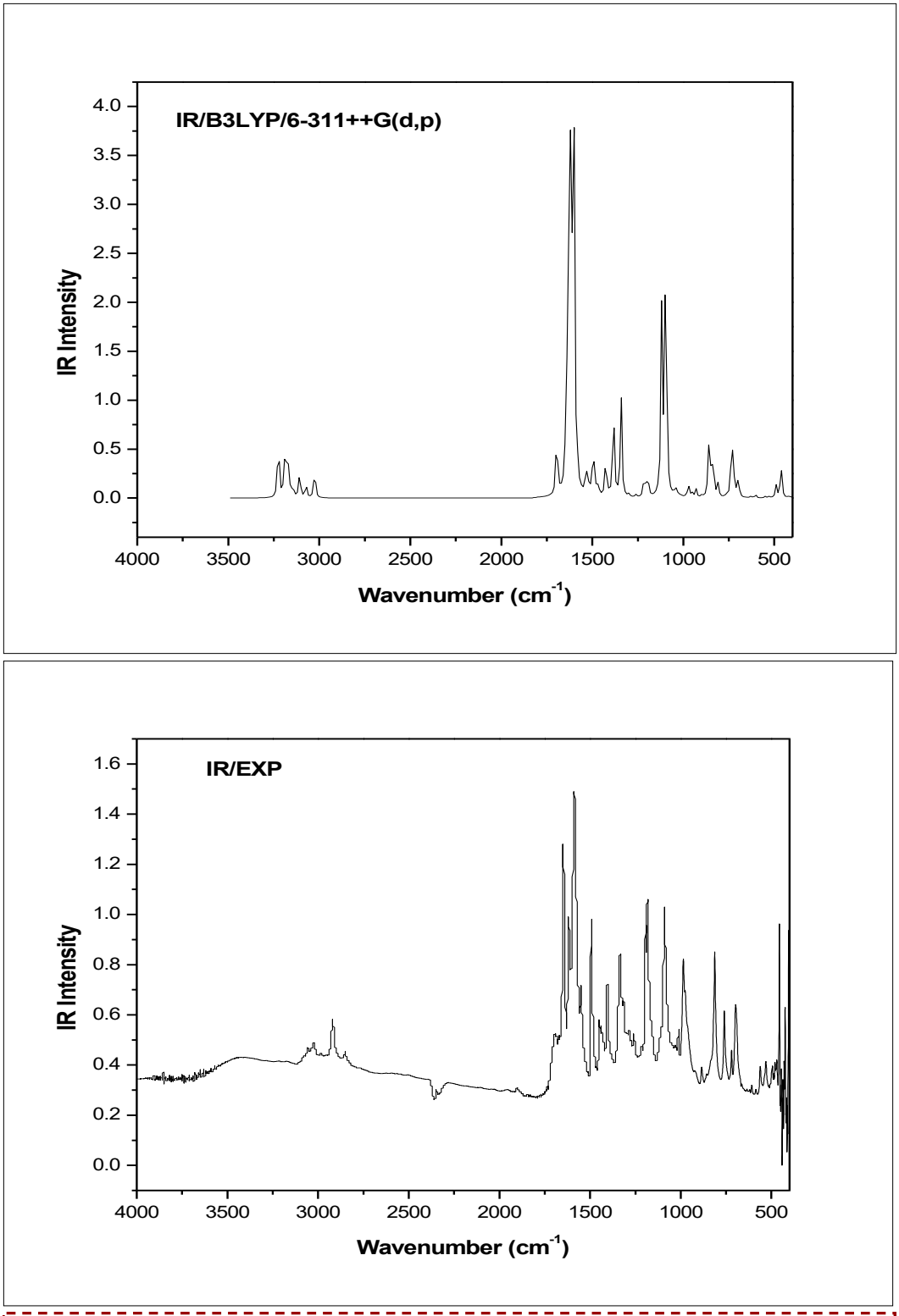

Fig. 2. The combined theoretical and experimental FT-IR spectra of MPPO

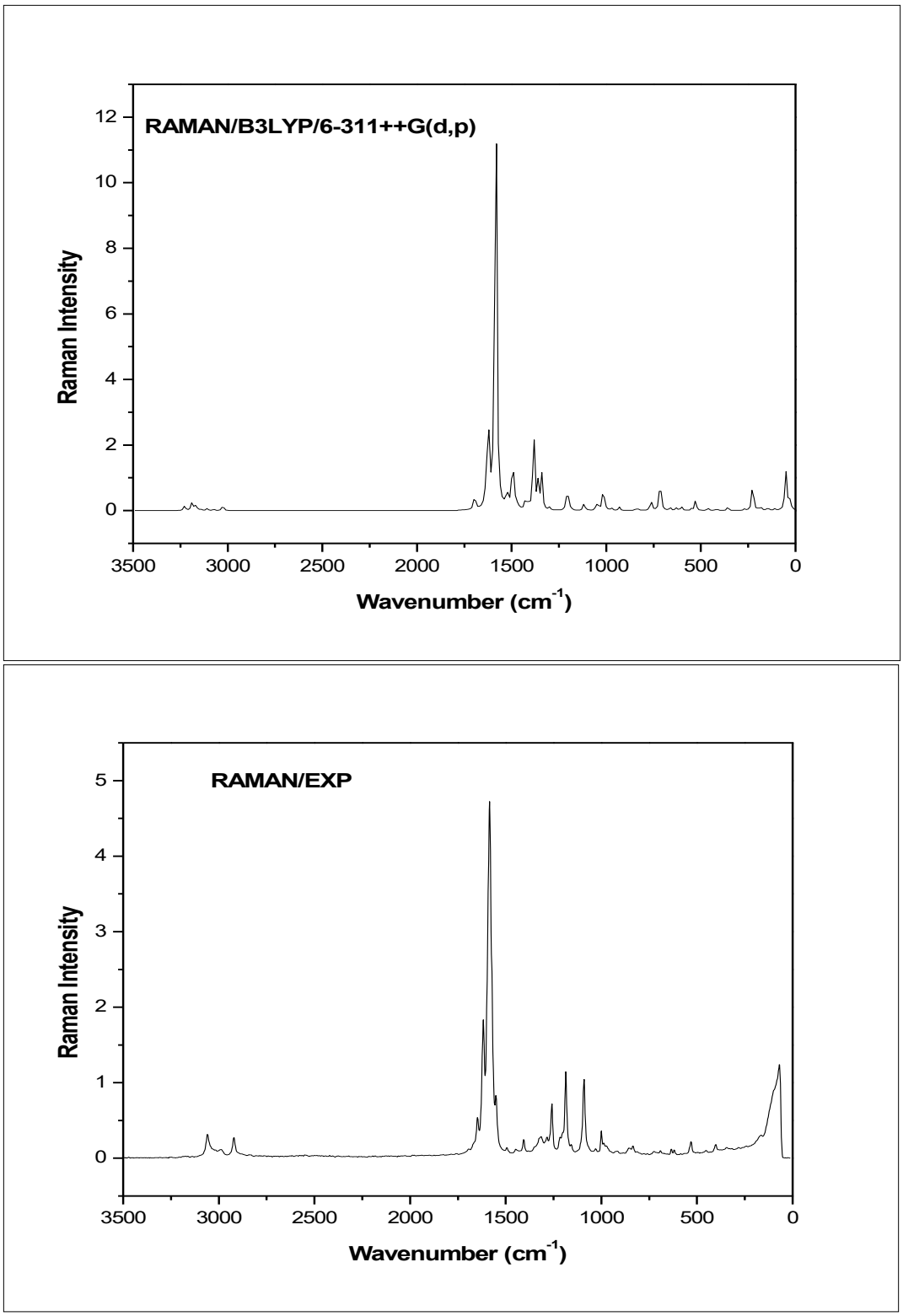

Fig. 3. The combined theoretical and experimental FT-Raman spectra of MPPO

(CH_3asym. stretching); the symmetrical (CH_3 sym. deformation) and anti-symmetrical (CH_3asy. deformation) deformation modes; the in-plane rocking (CH_3ipr), out-of-plane rocking (CH_3opr) and twisting (CH_3) bending modes. The asymmetric/symmetric CH stretching modes of CH_3 are expected in the region around 2980/2870 cm^{-1}, respectively [36-39]. The CH_3asy/sym frequencies are established at 3068, 3063/3052 cm^{-1} (mode nos: 3, 4/5), respectively. This assignment is further supported by observed bands (FTIR: 3064/FT-Raman: 3059 cm^{-1}) in addition to TED values (>83%). The asymmetric/symmetric CH_3 bending vibrations usually occur in the regions 1430-1470cm^{-1}/1360-1400 cm^{-1}, respectively [40]. In accordance with the above literature, the harmonic bands 1445, 1432/1357cm^{-1} (mode nos: 22, 24/28) are respectively assigned to βasy CH/βsy CH of CH_3 group. Further, these assignments are supported from observed FTIR band: 1447 cm^{-1} in addition to TED values (>60%).

The CH_3 rocking modes usually appeared[39]in the region 1010-1070 cm^{-1}. The bands established at 983 and 966 cm^{-1} in FT-Raman and FTIR were assigned to CH_3 in-plane and out-of-plane rocking modes, respectively [41]. The value of these bands are calculated at 1010 and 998 cm^{-1} (mode nos: 43 and 44) with considerable TED values (68% & 40%). The mode no: 44 coincideswith observed FT-Raman band (1000 cm^{-1}). These assignments find support from the literatureSubramanian et al., [42] and were within the frequency intervals given by Varsanyi et al.,[43]. The CH_3 torsional mode was assigned at 168 cm^{-1}[42]. It should be mentioned here, that this mode is pure with 95% TED value. Hence the mode no: 85 is undoubtedly assigned to τCH_3 mode.

C=C, C-C Vibrations

The ring C=C and C-C stretching vibrationsknown as semicircle stretching usually occur in the region 1450–1625 cm^{-1}[44, 45]. Varsanyi et al., [46] have assigned the ν_{C-C} vibrations in the regions of 1590-1625,1575-1590,1470-1540,1430-1460 and 1280-1380cm^{-1} with variable intensity of bands. The ring ν_{C-C}modes occur in the region 1530-1625cm^{-1}[42].In this region there are two (or) three bands due to skeletal vibrations, the strongest usually being at about 1500cm^{-1} for aromatic six member rings. Hence, the bands of strong to medium intensity in FTIR at1617 (m),1586 (vs) & 1012 (m) cm^{-1} and FT-Raman at 1616(w),1584 (vs),1314(w) & 1258 (w) cm^{-1} are assigned to C-C stretching vibrations of benzene moiety. The frequencies assigned to vC-C modes agree well with the literature [44, 45] and also in line with the harmonic wavenumbers in the range 1578-976cm^{-1}(mode nos:16,17,31,33,42, 47) in addition to TED values.

The β_{CCC} and Γ_{CCC}modes are associated with smaller force constant than the stretching one and hence assigned to lower frequencies. The β_{CCC} modes of benzene ring are expected to appear with considerable intensity under the reduced symmetry.The C-C-C in-plane bending vibrations can be observed in the FTIR spectrum at 1012cm^{-1} and in FT-Raman spectrum at 634 cm^{-1}.Similarly the C-C-C out-of-plane bending modes can be observed as a medium band in FTIR spectrum at 455cm^{-1}. These results are supported by computed wavenumbers 1011, 976, 637 and 670, 505, 470 cm^{-1} (mode nos:42, 47, 65 and 64, 71,72), respectively in addition to literature values [39].

Literature survey reveals that the C-C stretching vibrations in substituted thiophen rings were reported in ranges of 1329-1431,1420-1501 and 1419-1519cm^{-1} [28,30, 31]. Inour case the very strong bands at

1586/1584 cm^{-1} in FTIR/FT-Raman and harmonic bands at 1560, 1370 and 1148 cm^{-1}(mode nos:17,27 &37) are assigned to ν_{C-C} modes in MPPO. These assignments are having considerable TED values(>24%). As it is evident from the Table2, the β_{CCC} modes: 811,687 cm^{-1}(mode nos:56,63) are mixed with ν_{C-S} modes. Mode no: 56 is in good agreement with observed FTIR band at 812cm^{-1} in addition to TED output (>15%). These assignments are also in accordance with literature[28,30& 31]. The mode nos:67,79 (601, 228cm^{-1}) are designated as Γ_{CCC} modes of thiophen moiety with considerable TED values (>58%).

The harmonic frequencies established at 1541,1474,1330,1075 cm^{-1}(mode nos: 18,20,29,39) and 1158cm^{-1}, (mode no:36) are attributed to ν_{CC} modes of pentadiene moietyand νC_{20}-C_{22},νC_1-C_{12} modes, respectively. These assignments are having considerable TED values (>25%) and also find support from the observed bands:1550,1492, 1334,1090 cm^{-1} (FTIR)/1551,1494,1090 cm^{-1} FT-Raman. The mode no:34 (1212/1193cm^{-1}:FTIR) is attributed νC_2-C_8 mode. The harmonic wavenumbers:894,607,528, 445 cm^{-1} (mode nos:52,66,69,73) and 689,737,336cm^{-1}(mode nos:62,59,77) are respectively assigned to β_{CCC} and τ_{CCC} modes of pentadiene, in which mode nos:69,73 and 62 are agreeable with observed bands: (FT-Raman/FTIR) 531/424cm^{-1} and 691/697cm^{-1}. These assignment are also having considerable TED values.

C-H Vibrations

The ν_{C-H} modes of hetero aromatic structure are expected to occur in the range of 3000-3100cm^{-1} with some weak bands. The vibrational band in this region are not affected appreciably by the nature of the substituent's [43, 44]. In MPPO,the weak bands at 2919 (2921:FT-Raman), 2843cm^{-1} in FTIR spectrum have been assigned to ν_{C-H} vibrations. The present theoretical calculation by B3LYP/6-311++G(d,p) method places this modes at 3104,3041,2984,2953,2907cm^{-1} (mode nos:1,7,12,13,14). This shows that the bands have appeared at the expected position of the spectra, except the last band (2843cm^{-1}) which is slightly less.The reduction in the frequency value is naturally due to the presence of CH_3 group inMPPO.

In aromatic compounds the C-H in-plane /out-of -plane bending frequencies appear in the ranges of 1000 -1300/750-1000cm^{-1}, respectively[45,46]. In this work the β_{C-H} modes are assigned in the range 1307-1011cm^{-1} (modenos:31,33,35,38,42), which are in agreement with observed bands in FTIR at 1183,1012 cm^{-1} and in FT-Raman at 1314,1258,1185 cm^{-1}. The calculated frequencies 991-777cm^{-1} (mode nos: 45, 49, 51, 55, 58) for C-H out-of-plane bending modes fall in the FTIR values of 985,760cm^{-1}. These assignments are find support from the Varsanyi [46] and also find support from TED values. Hence, among the CH vibrations, only the CH stretching modes are found influenced by the substitutional group, whereas the β_{CH} and Γ_{CH}modes are remain unaffected.

The C-H stretching modes are expected to appear with multiple weak bands in the frequency range 3000-3100cm^{-1}. These bands are not affected appreciably by the nature of the substituent's [43, 47].The ν_{C-H} modes were observed at 3011,3062 and 3072 cm^{-1} in FTIR spectrum by Balachandran et al., [31]. Based on the above conclusion, the calculated frequencies 3027,2989cm^{-1} (mode nos: 9, 11) are assigned to ν_{C-H} vibrations of thiophen moiety. These assignments are aggreable with observed FTIR band at 3021 cm^{-1} and also find support from TED values

(>75%).The C-H in-plane bending modes appeared by sharp but weak to medium bands in the range 1100-1500cm^{-1} and the bands were not sensitive to the nature of substitutent's. The Γ_{C-H} out-of-plane bending modes were expected to occur in the region 800-1000cm^{-1} [47].With reference to this, the observed medium band at 1193cm^{-1} in FTIR is attributed to β_{C-H} of thiophen ring. For the same mode the theoretical frequencies are:1370,1212cm^{-1} (mode nos:27,34). The harmonic wavenumbers:1066 and 862, 705cm^{-1} (mode nos:40 and 53,61) are designated as β_{HCS} and τ_{HCCS} modes, respectively and theseassignments have considerable TED values (>50%).

In this work, it has been established well and the calculated wavenumbers in the range 3098-3016cm^{-1} (mode nos:2,6,8,10) are designated as ν_{C-H} modes of pentadiene moiety[46,47]. For this mode, the corresponding vibrational bands are missing in the experimental spectra, which may be dueto isomer. Hence, the above assignments are justified with the help of TED values (>72%).The β_{C-H} modes are attributed to the FTIR/FT-Raman bands present at 1404/1406cm^{-1} and for the same mode the harmonic frequencies are 1464,1437,1428,1409cm^{-1}(mode nos: 21,23,25,26). This assignment is aggreable with literature [47]in addition to TED results (>42%). The τ_{CCCH} vibrations are characterized by the FT-Raman/FTIR bands at 834,691/697cm^{-1},while the calculated wavenumbers are: 979, 958,831,825,689cm^{-1}(mode nos:46,48,54,55,62) and also have considerable TED values (>42%).

NLO Property

The total dipole moment and first-order hyperpolarizability (β_0) of MPPO is calculated by using B3LYP/6-311++G(d,p) basis set and are listed in Table.3.The calculated dipole moment and the mean first hyperpolarizability (β_0) values are 0.7071 Debye and 10.2328x10^{-30} esu, respectively, and the values are presented in Table3. Total hyperpolarizability of the title molecule is approximately twenty seven times greater than that of urea. The above results show that MPPO can be best material for NLO applications.

NBO Analysis

The NBO analysis is performed on MPPO using B3LYP/6-311++G(d,p) basis set. The $E^{(2)}$ energies and types of interactions are listed in Table 4.The EDs of the conjugated single as well as double bond of the aromatic/thiophene rings are 1.979& 1.606e/1.979&1.773e,respectively.This exhibits a strong delocalization inside the molecule MPPO. The non-bonding atoms transfer more energy to the acceptor, during the intra-molecular interactions. The LP(2) S_5 and LP(2) O_{17} atoms transfer more energy (27.15 and 14.61 KJ/mol) to anti-bonding orbitals C_3-C_4 and C_{14}-C_{16}, respectively, when compare with σ-σ* transition for the same. These interactions causes a pronounced and moderate decrease of the lone pair orbitals occupancies; 1.581e and 1.886e, respectively, and there is a possibility for hyperconjugativeinteraction between them.The donor and acceptor interactions of πC_{22}-$C_{24}\rightarrow\pi^*C_{23}$-$C_{25}$(20.9 KJ/mol); πC_{27}-$C_{29}\rightarrow\pi^*C_{23}$-$C_{25}$ (18.55KJ/mol) reveal the maximum hyperconjugative interaction in benzene ring of MPPO.

Homo-Lumo Analysis

Molecular orbital and their properties like energy are very useful to the physicists and chemists [44]. The HOMO acts as an electron donor and the LUMO is the electron acceptor, and the gap between HOMO and

Table 3. The NLO measurements of MPPO.

Parameters	B3LYP/6-311++G(d,p)
Dipole moment (μ)	Debye
μ_x	-0.4885
μ_y	0.5112
μ_z	0.0001
μ	0.7071 Debye
Polarizability (α_0)	*x10^{-30}esu*
α_{xx}	418.01
α_{xy}	4.69
α_{yy}	237.33
α_{xz}	-0.01
α_{yz}	0
α_{zz}	113.8
α_0	0.69x10^{-30}esu
Hyperpolarizability (β_0)	x*10^{-30}esu*
β_{xxx}	284.46
β_{xxy}	804.11
β_{xyy}	107.07
β_{yyy}	306.1
β_{xxz}	0.02
β_{xyz}	-0.01
β_{yyz}	0.06
β_{xzz}	22.34
β_{yzz}	-0.42
β_{zzz}	0.0044
β_0	10.23x10^{-30}esu

Standard value for urea (μ=1.3732 Debye, β0=0.3728x10-30esu): esu-electrostatic unit

Table 4. The second order perturbation theory analysis of Fock Matrix in NBO basis for MPPO

Type	Donor NBO (i)	ED/e	Acceptor NBO (j)	ED/e	$E^{(2)}$ KJ/mol	E(j)-E(i) a.u.	F(i,j) a.u.
σ-σ*	BD (1) C 1 - C 2	1.97397	BD*(1) C 1 - C 12	0.0274	3.73	1.22	0.06
			BD*(1) C 12 - C 14	0.01462	1.94	1.96	0.055
π-π*	BD (2) C 1 - C 2	1.73778	BD*(2) C 3 - C 4	0.32831	16.62	0.27	0.06
			BD*(1) C 8 - H 10	0.00953	1.87	0.66	0.034
			BD*(1) C 8 - H 11	0.00953	1.87	0.66	0.034
			BD*(2) C 12 - C 14	0.17953	20.25	0.33	0.074
σ-σ*	BD (1) C 1 - S 5	1.97486	BD*(1) C 4 - H 7	0.01311	2.76	1.22	0.052
			BD*(1) C 12 - H 13	0.01378	1.76	1.08	0.039
σ-σ*	BD (1) C 1 - C 12	1.97917	BD*(1) C 12 - C 14	0.01462	1.53	1.96	0.049
			BD*(1) C 14 - H 15	0.01324	1.42	1.16	0.036
			BD*(1) C 16 - C 18	0.05908	34.4	0.24	0.082
			BD*(1) C 18 - H 19	0.01254	120.55	0.08	0.09
			BD*(1) C 22 - C 24	0.02627	27.23	0.32	0.083
			BD*(2) C 22 - C 24	0.36662	36.29	0.13	0.067
σ-σ*	BD (1) C 2 - C 3	1.97199	BD*(1) C 1 - C 12	0.0274	4.38	1.19	0.065
			BD*(1) C 3 - C 4	0.01512	2.83	1.36	0.056
			BD*(1) C 4 - H 7	0.01311	3.02	1.25	0.055
σ-σ*	BD (1) C 2 - C 8	1.97883	BD*(1) C 3 - C 4	0.01512	1.28	1.32	0.037
σ-σ*	BD (1) C 3 - C 4	1.98319	BD*(1) C 4 - H 7	0.01311	1.34	1.3	0.037
π-π*	BD (2) C 3 - C 4	1.8072	BD*(2) C 3 - C 4	0.32831	0.65	0.28	0.012
σ-σ*	BD (1) C 3 - H 6	1.97779	BD*(1) C 3 - C 4	0.01512	1.33	1.21	0.036
σ-σ*	BD (1) C 4 - S 5	1.97845	BD*(1) C 1 - C 12	0.0274	4.22	1.18	0.063
σ-σ*	BD (1) C 4 - H 7	1.98573	BD*(1) C 3 - C 4	0.01512	1.3	1.23	0.036
			BD*(1) C 16 - C 18	0.05908	13.02	0.08	0.03
			BD*(1) C 22 - C 24	0.02627	7.54	0.16	0.031
σ-σ*	BD (1) C 8 - H 9	1.98812	BD*(1) C 12 - C 14	0.01462	3.95	1.87	0.077
			BD*(1) C 16 - O 17	0.01724	4.38	1.27	0.067
			BD*(1) C 24 - H 28	0.02271	2.98	1.1	0.051
			BD*(2) C 27 - C 29	0.33144	2.97	3.85	0.104
			BD*(1) C 27 - H 31	0.01409	2.52	4.81	0.098
σ-σ*	BD (1) C 8 - H 10	1.9793	BD*(1) C 22 - C 24	0.02627	74.35	0.12	0.086
σ-σ*	BD (1) C 12 - H 13	1.96197	BD*(1) C 14 - H 15	0.01324	1.05	0.96	0.029
			BD*(1) C 14 - C 16	0.05431	5.72	1.06	0.07
σ-σ*	BD (1) C 12 - C 14	1.98129	BD*(1) C 1 - C 12	0.0274	4.63	1.25	0.068
			BD*(1) C 14 - C 16	0.05431	2.42	1.28	0.05
			BD*(1) C 16 - C 18	0.05908	8.93	0.27	0.044

Type	Donor NBO (i)	ED/e	Acceptor NBO (j)	ED/e	$E^{(2)}$ KJ/mol	E(j)-E(i) a.u.	F(i,j) a.u.
π-π*	BD (2) C 12 - C 14	1.81895	BD*(2) C 16 - O 17	0.27328	21.41	0.29	0.072
σ-σ*	BD (1) C 14 - H 15	1.97581	BD*(1) C 1 - C 12	0.0274	7.09	1.02	0.076
			BD*(1) C 16 - O 17	0.01724	3.76	1.16	0.059
σ-σ*	BD (1) C 14 - C 16	1.9799	BD*(1) C 12 - H 13	0.01378	1.96	1.09	0.041
			BD*(1) C 12 - C 14	0.01462	2.04	1.91	0.056
			BD*(1) C 16 - C 18	0.05908	5.72	0.19	0.03
			BD*(1) C 18 - H 19	0.01254	4.58	0.03	0.011
σ-σ*	BD (1) C 16 - O 17	1.99368	BD*(1) C 16 - C 18	0.05908	2.76	0.57	0.036
π-π*	BD (2) C 16 - O 17	1.96036	BD*(2) C 12 - C 14	0.17953	4.25	0.43	0.039
			BD*(2) C 18 - C 20	0.13135	4.57	0.4	0.039
σ-σ*	BD (1) C 16 - C 18	1.98102	BD*(1) C 12 - C 14	0.01462	1.59	1.91	0.049
			BD*(1) C 18 - H 19	0.01254	6.35	0.03	0.012
			BD*(1) C 20 - H 21	0.01242	1.68	1.09	0.038
σ-σ*	BD (1) C 18 - H 19	1.97184	BD*(1) C 16 - O 17	0.01724	4.69	1.15	0.066
			BD*(1) C 20 - H 21	0.01242	1.26	0.94	0.031
			BD*(1) C 20 - C 22	0.02819	7.7	1	0.078
σ-σ*	BD (1) C 18 - C 20	1.98216	BD*(1) C 16 - C 18	0.05908	14.3	0.27	0.056
			BD*(1) C 18 - H 19	0.01254	8.42	0.11	0.028
			BD*(1) C 20 - C 22	0.02819	3.69	1.23	0.06
π-π*	BD (2) C 18 - C 20	1.84033	BD*(2) C 16 - O 17	0.27328	20.32	0.29	0.07
σ-σ*	BD (1) C 20 - H 21	1.97149	BD*(1) C 16 - C 18	0.05908	73.62	0.05	0.056
			BD*(1) C 22 - C 24	0.02627	40.86	0.13	0.065
σ-σ*	BD (1) C 20 - C 22	1.97691	BD*(1) C 16 - C 18	0.05908	9.02	0.2	0.038
			BD*(1) C 22 - C 23	0.02207	2.06	1.22	0.045
			BD*(1) C 22 - C 24	0.02627	32.81	0.27	0.085
			BD*(2) C 22 - C 24	0.36662	7.71	0.08	0.025
σ-σ*	BD (1) C 22 - C 23	1.97392	BD*(1) C 20 - C 22	0.02819	2.17	1.17	0.045
			BD*(2) C 22 - C 24	0.36662	120.04	0.1	0.106
σ-σ*	BD (1) C 22 - C 24	1.9728	BD*(1) C 23 - H 26	0.0143	3.64	1.12	0.057
			BD*(1) C 24 - C 27	0.01547	2.59	1.27	0.051
π-π*	BD (2) C 22 - C 24	1.5862	BD*(2) C 18 - C 20	0.13135	13.05	0.29	0.059
			BD*(2) C 23 - C 25	0.31148	20.9	0.29	0.071
			BD*(2) C 27 - C 29	0.33144	2.84	3.47	0.09
σ-σ*	BD (1) C 23 - C 25	1.97917	BD*(1) C 4 - H 7	0.01311	3.66	1.28	0.061
			BD*(1) C 20 - C 22	0.02819	3.26	1.21	0.056
			BD*(1) C 22 - C 23	0.02207	4.39	1.27	0.067
σ-σ*	BD (1) C 23 - H 26	1.98069	BD*(1) C 22 - C 23	0.02207	0.69	1.07	0.024
σ-π*	BD (1) C 24 - C 27	1.97888	BD*(2) C 3 - C 4	0.32831	3.77	0.9	0.056
			BD*(1) C 4 - H 7	0.01311	6.05	1.47	0.084
			BD*(1) C 16 - O 17	0.01724	4.9	1.55	0.078
			BD*(1) C 20 - C 22	0.02819	4.41	1.39	0.07
σ-σ*	BD (1) C 24 - H 28	1.97705	BD*(1) C 16 - C 18	0.05908	27.9	0.02	0.023

Type	Donor NBO (i)	ED/e	Acceptor NBO (j)	ED/e	$E^{(2)}$ KJ/mol	E(j)-E(i) a.u.	F(i,j) a.u.
			BD*(1) C 22 - C 23	0.02207	4.86	1.05	0.064
			BD*(1) C 22 - C 24	0.02627	27.94	0.1	0.048
σ-π*	BD (1) C 25 - C 29	1.97941	BD*(2) C 3 - C 4	0.32831	4.09	0.69	0.052
			BD*(1) C 12 - C 14	0.01462	10.22	1.94	0.126
			BD*(1) C 16 - O 17	0.01724	9.45	1.34	0.101
			BD*(1) C 23 - H 26	0.0143	6.31	1.13	0.075
			BD*(1) C 24 - H 28	0.02271	8.21	1.17	0.087
σ-σ*	BD (1) C 25 - H 30	1.98016	BD*(1) C 4 - H 7	0.01311	3.33	1.1	0.054
			BD*(1) C 22 - C 23	0.02207	5.6	1.08	0.069
			BD*(1) C 24 - H 28	0.02271	3.22	1	0.051
			BD*(1) C 29 - H 32	0.01371	2.72	2.61	0.075
σ-π*	BD (1) C 27 - C 29	1.98062	BD*(2) C 3 - C 4	0.32831	4.13	0.69	0.052
			BD*(1) C 12 - C 14	0.01462	9.11	1.94	0.119
			BD*(1) C 16 - O 17	0.01724	9.4	1.34	0.1
			BD*(2) C 27 - C 29	0.33144	16.2	3.92	0.245
π-π*	BD (2) C 27 - C 29	1.64275	BD*(2) C 23 - C 25	0.31148	18.55	0.29	0.066
σ-σ*	BD (1) C 27 - H 31	1.98023	BD*(1) C 4 - H 7	0.01311	3.3	1.08	0.053
			BD*(1) C 24 - H 28	0.02271	5.55	0.99	0.066
σ-π*	BD (1) C 29 - H 32	1.98091	BD*(2) C 3 - C 4	0.32831	4.65	0.48	0.046
			BD*(1) C 12 - C 14	0.01462	26.51	1.73	0.191
			BD*(1) C 16 - O 17	0.01724	16.8	1.13	0.123
			BD*(1) C 24 - H 28	0.02271	9.57	0.96	0.086
			BD*(2) C 27 - C 29	0.33144	23.61	3.71	0.288
			BD*(1) C 27 - H 31	0.01409	34.65	4.66	0.359
n-σ*	LP (1) S 5	1.98351	BD*(1) C 3 - C 4	0.01512	2.25	1.32	0.049
n-π*	LP (2) S 5	1.58098	BD*(2) C 3 - C 4	0.32831	27.15	0.24	0.074
n-σ*	LP (1) O 17	1.969	BD*(1) C 14 - C 16	0.05431	2.03	1.23	0.045
			BD*(1) C 16 - C 18	0.05908	5.78	0.22	0.032
			BD*(1) C 24 - H 28	0.02271	2.57	1.16	0.049
n-π*	LP (2) O 17	1.88598	BD*(1) C 14 - C 16	0.05431	14.61	0.81	0.098
			BD*(1) C 24 - H 28	0.02271	2.64	0.74	0.04
π*-σ*	BD*(2) C 1 - C 2	0.39784	BD*(1) C 12 - C 14	0.01462	8.28	33.56	1.036
			BD*(1) C 16 - O 17	0.01724	8.11	32.96	1.013
			BD*(2) C 27 - C 29	0.33144	21.31	35.54	1.286
			BD*(1) C 27 - H 31	0.01409	8.56	36.49	1.099

Type	Donor NBO (i)	ED/e	Acceptor NBO (j)	ED/e	$E^{(2)}$ KJ/mol	E(j)-E(i) a.u.	F(i,j) a.u.
			BD*(1) C 29 - H 32	0.01371	4.11	34.39	0.74
π*-π*	BD*(2) C 3 - C 4	0.32831	BD*(2) C 16 - O 17	0.27328	0.71	0.02	0.005
π*-σ*	BD*(2) C 12 - C 14	0.17953	BD*(1) C 29 - H 32	0.01371	2.9	2.02	0.22
π*-π*	BD*(2) C 16 - O 17	0.27328	BD*(2) C 12 - C 14	0.17953	35.93	0.05	0.077
			BD*(2) C 18 - C 20	0.13135	62.96	0.02	0.074
π*-π*	BD*(2) C 18 - C 20	0.13135	BD*(2) C 27 - C 29	0.33144	1.45	3.19	0.126
π*-π*	BD*(2) C 22 - C 24	0.36662	BD*(2) C 3 - C 4	0.32831	5.26	0.58	0.084
			BD*(1) C 16 - O 17	0.01724	3.86	1.23	0.141
			BD*(2) C 23 - C 25	0.31148	6.92	0.62	0.101
			BD*(1) C 24 - H 28	0.02271	3.37	1.06	0.121
π*-π*	BD*(2) C 23 - C 25	0.31148	BD*(2) C 27 - C 29	0.33144	6.83	3.19	0.232
π*-σ*	BD*(2) C 27 - C 29	0.33144	BD*(1) C 27 - H 31	0.01409	367.87	0.96	1.273

a E(2) means energy of hyper conjugative interaction (stabilization energy).

b Energy difference between donor (i) and acceptor(j) nbo orbitals.

c F(i,j) is the Fock matrix element between i and j nbo orbitals.

Table 5. The Physico-chemical properties of MPPO

Parameters	Values
HOMO	-6.055 eV
LUMO	-2.622 eV
Energy gap	3.432 eV
Ionization potential (IP)	6.055 eV
Electron affinity (EA)	2.622 eV
Electrophilicity Index (ω)	2.741
Chemical Potential (μ)	4.338
Electronegativity (χ)	4.338
Hardness (η)	-3.432
Softness (S)	6.866

LUMO characterizes the molecular chemical stability. The energy gap between the HOMO and the LUMO MOs is a critical parameter in determining molecular electrical transport properties because it is a measure of electron conductivity. Fig.4 shows, the HOMO-LUMO plots of MPPO. The HOMO is located over the thiophen ring and partly on CH_3 group. The LUMO located all over the molecule except methyl group, since methyl group has large electronegativity. The energy gap of MPPO molecule is calculated as 3.4327 eV in gas phase using B3LYP/6-311++G(d,p) basis set.HOMO implies the energy of about -6.0551 eV and LUMO energy is -2.6224 eV. The various physico-chemical parameters are listed in Table.5 and the frontier molecular orbital energies are also listed in Table 6.

UV-Vis Spectra

The electronic spectra of the title moleculeis calculated using TD-DFT/B3LYP/6-311++G(d,p) basis set. The electronic transitions, positions of experimental absorption peaks, calculated absorption peaks (λ_{max}), vertical excitation energies, oscillator strengths (f) are listed in Table7. The observed and UV-Vis absorption maximum of MPPO are shown in Fig.5.In this study, the electronic transition is calculated at three excited states (ES) like as ES_1, ES_2 and ES_3, respectively,in which ES_1 appeared at 421.19nm (2.9436eV), ES_2 at 398.42 nm (3.1119eV) and ES_3 lies at 343.32nm (3.6113eV). In ES_3 state there are three transitions from HOMO 64 to Lumo 68, HOMO66 to LUMO68 and HOMO 67 to LUMO 69. The molecule MPPO has sulphur and oxygen as lone pairs, hence π-π* transition is also possible.The electronic absorption calculation shows that the visible absorption maximafor MPPO corresponds to the electron transition between frontier orbitals such as transition from HOMO to LUMO. It should be mentioned here that the low energy absorptions is found at 303 nm and 352 nm belong to the dipole allowed σ-σ* and π-π* transition from HOMO to LUMO, respectively. The intense bands calculated at 398nm can be assigned to high delocalization of π-electrons in the thiophen moiety of MPPO. Similarly the intense band at 343nm can be distributed to the excitation of σ-electrons which are localized on the whole molecular system.

MEP Analysis

MEP indicates the net electrostatic effect produced at that point by the total charge distribution (nuclei + electron) of the molecule and correlates with dipole moments, electronegativity, partial charges and chemical reactivity of the molecules. It provides a visual method to understand the relative polarity of the molecule. The different values of the electrostatic potential represented by different colors; red represents the regions of the most negative electrostatic potential, blue represents the regions of the most positive

Table 8. The Mulliken atomic charges of MPPO

Atoms	Charges	Atoms	Charges
1C	0.519	17O	-0.2251
2C	0.0009	18C	-0.3645
3C	-0.2145	19H	0.1716
4C	-0.0636	20C	-0.2478
5S	-0.5428	21H	0.1456
6H	0.1464	22C	0.9651
7H	0.2521	23C	0.1338
8C	-0.9824	24C	-0.7922
9H	0.1601	25C	-0.3845
10H	0.1602	26H	0.1524
11H	0.1602	27C	-0.1456
12C	0.219	28H	0.1564
13H	0.1608	29C	-0.1516
14C	-0.1696	30H	0.1636
15H	0.1724	31H	0.1782
16C	0.1067	32H	0.1589

Table 6. The frontier molecular orbitals of MPPO

Occupancy	Orbital energies (a.u)	Orbital energies (eV)	Kinetic energies (a.u)
O_{52}	-0.269	-7.343	1.118
O_{53}	-0.252	-6.858	2.314
O_{54}	-0.246	-6.708	1.429
O_{55}	-0.241	-6.569	1.348
O_{56}	-0.235	-6.405	1.388
V_{57}	-0.097	-2.646	1.398
V_{58}	-0.051	-1.397	1.289
V_{59}	-0.025	-0.694	1.244
V_{60}	0.016	-0.441	1.358
V_{61}	0.013	-0.373	0.251

Table 7. The electronic transitions of MPPO

Calculated at B3LYP/6-311++G(d,p)	Oscillator Strength	Calculated Band gap(ev/nm)	Experimental Type Band gap (ev/nm)
Excited State-1	Singlet-A(f=0.0000)	2.9436 eV/421.19 nm	
65 -> 68	0.68512	4.164218	
Excited State-2	Singlet-A(f=0.6489)	3.6113 eV/343.32 nm	352 п–п*
67 -> 68	0.64129	3.432542	
Excited State-3	Singlet-A(f=0.0507)	3.6113 eV/343.32 nm	303 п –п*
64 -> 68	0.28196	4.289929	
66 -> 68	0.58917	3.960688	
67 -> 69	0.13934	4.689976	

Lumo = -2.622 eV

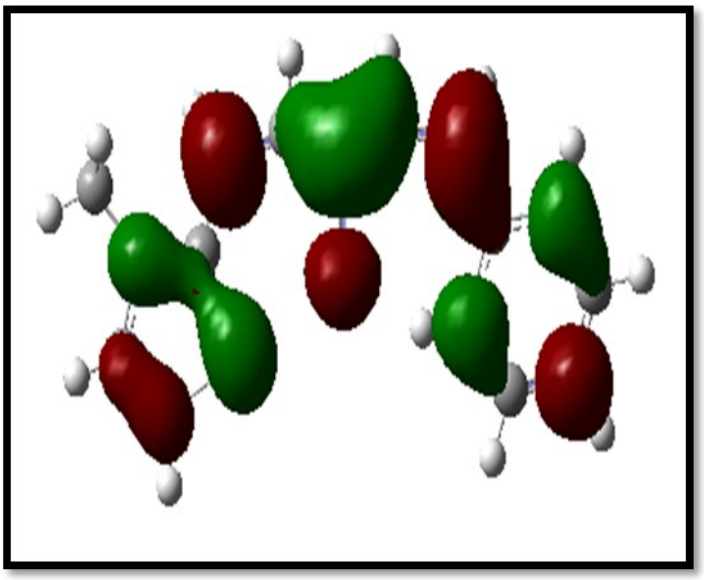

Energy gap = 3.432 eV

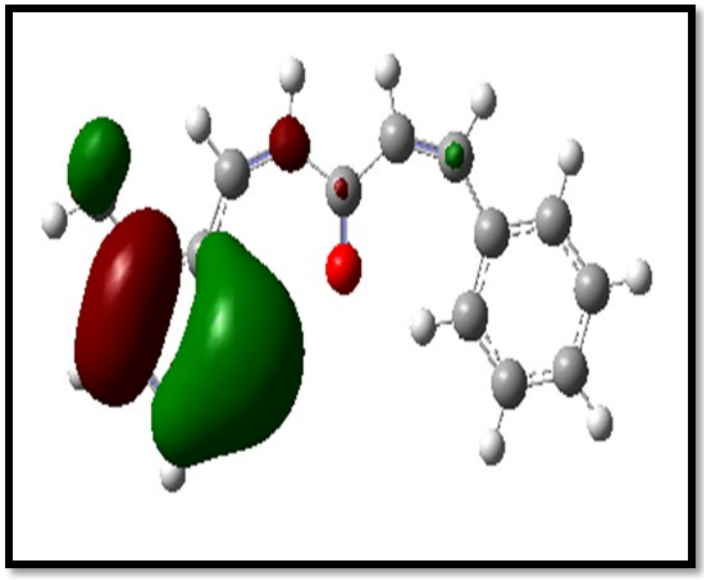

Homo = -6.055 eV

Fig. 4. The frontier molecular orbital of MPPO

Table 9. The calculated total energy (a.u), zero point vibrational energies (Kcal/mol), rotational constants (GHz) and entropy (cal/mol K-1) for MPPO

Parameters	B3LYP/6-311++G(d,p)
Total Energies	-1091.71
Zero-point Energy	158.198 (Kcal/Mol)
Rotational constants (GHZ)	1.013
	0.156
	0.135
Entropy	
Total	135.128
Translational	42.498
Rotational	33. 969
Vibrational	58.661

Table 10. Thermodynamic properties of MPPO at different temperatures

T (K)	S (J/mol.K)	Cp (J/mol.K)	ddH (kJ/mol)
100	376.62	119.6	8.02
200	481.8	194.81	23.62
298.15	575.09	278.44	46.82
300	576.82	280.01	47.34
400	668.56	359.67	79.42
500	756.18	425.73	118.81
600	838.65	478.52	164.12
700	915.71	520.88	214.17
800	987.59	555.43	268.04
900	1054.72	584.04	325.06
1000	1117.53	608.01	384.69

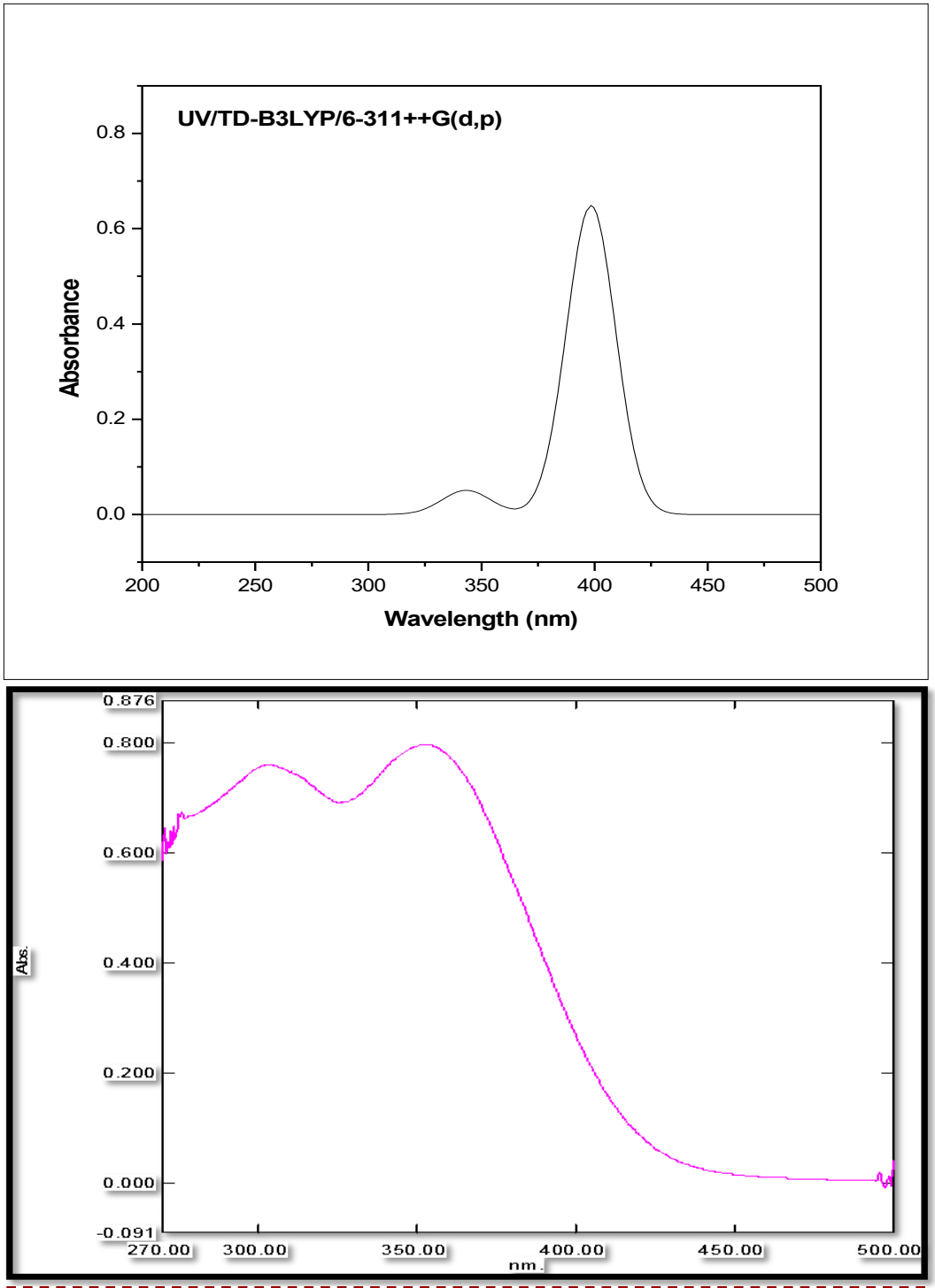

Fig. 5. The combined theoretical and experimental UV-Visible spectra of MPPO

electrostatic potential and green represents the regions of zero potential.The MEP is calculated with B3LYP/6-311++G(d,p) basis set and the MEP plot is shown in Fig.6.

The negative electrostatic potential corresponds to an attraction of the proton by the aggregate ED in the molecule (shades of red), while all the hydrogen atoms have positive electrostatic potential corresponds to the repulsion of the proton by the atomic nuclei (shades of blue). The MEP map shows that the negative region is mainly localized on oxygen and sulphur atoms while the positive region is localized on the surface of all the hydrogen atoms in MPPO. These regions indicate the active charge sites of the molecule. A region of zero potential envelopes the π-system of the aromatic rings [48].

Mulliken Charge Analysis

The calculation of atomic charges plays an important role in the application of quantum mechanical calculation to molecular system [49].The Mulliken charges of MPPO was calculated at B3LYP/6-311++G (d,p) level of theory and are listed in Table.8. The mulliken atomic charge plot is shown in Fig.7. The carbon atom (C_{22}) has more positive charge (0.9652 a.u), which isfused linkage with highelectronegative carbonyl group. Similarly,the methyl group carbon atom C_8 has maximum negative charge (-0.9825 a.u), sinceit isattached with thiophene ring. In MPPO all the hydrogen atoms have positive charge.

Thermodynamic Properties

The various thermodynamic parameter are computed by B3LYP/6-311++G(d,p) basis set and are listed in Table.9. The thermodynamic functions like heat capacity ($C^0_{p,m}$), entropy (S^0_m) and enthalpy changes (ΔH^0_m) are obtained from the theoretical harmonic frequencies. From Table.10, it can be seen that these thermodynamic functions are increasing with temperature ranging from 100 to 1000 K due to the fact that the molecular vibrational intensities increase with temperature [51]. The correlation equations between

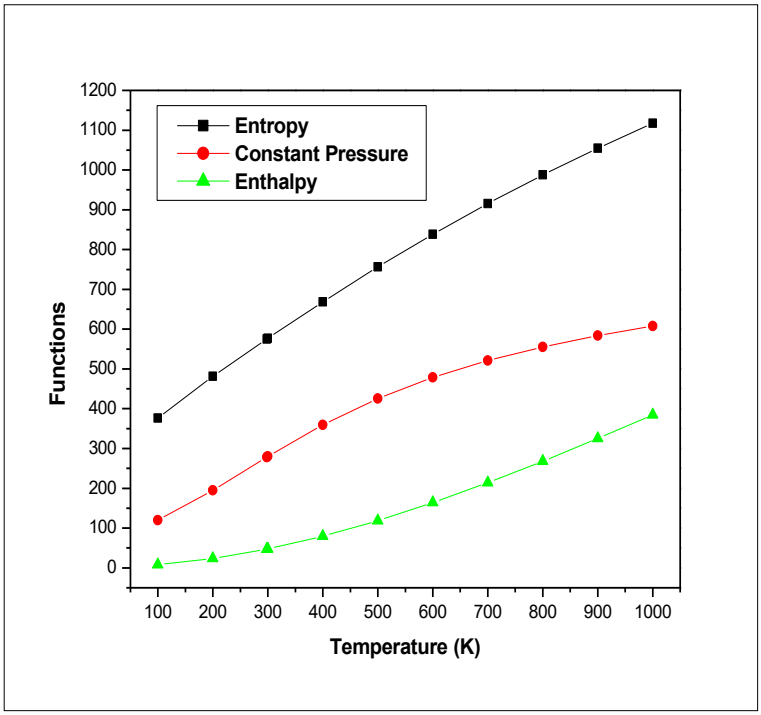

Fig. 8. The thermodynamic properties of MPPO at different

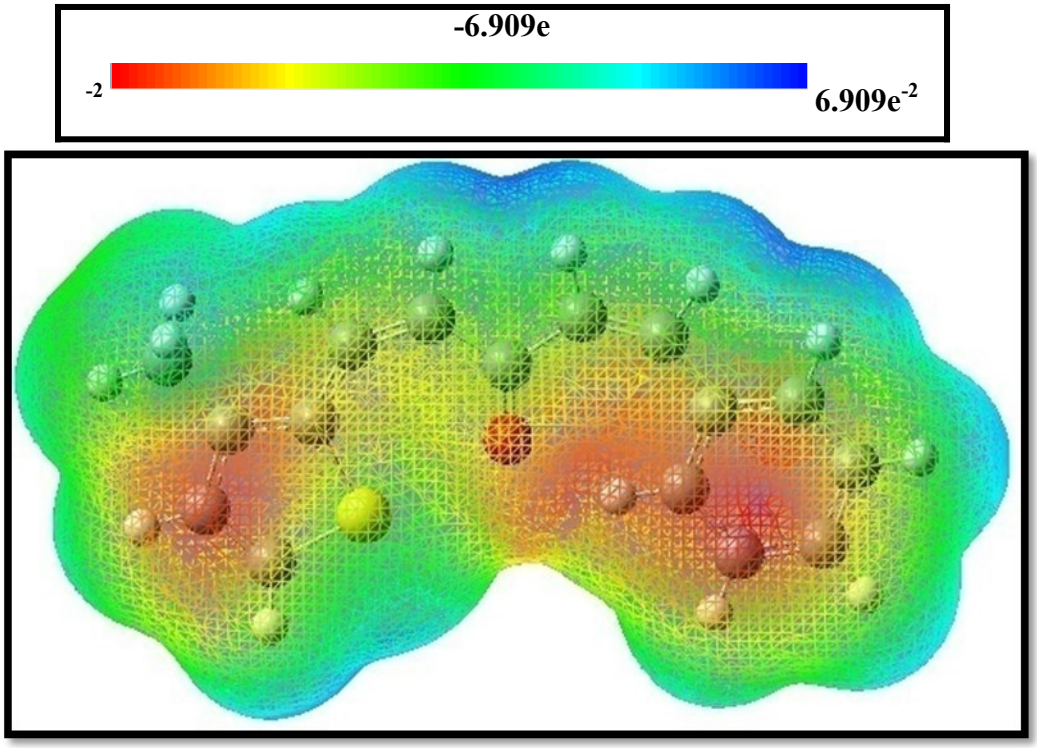

Fig.6. The molecular electrostatic potential map of MPPO

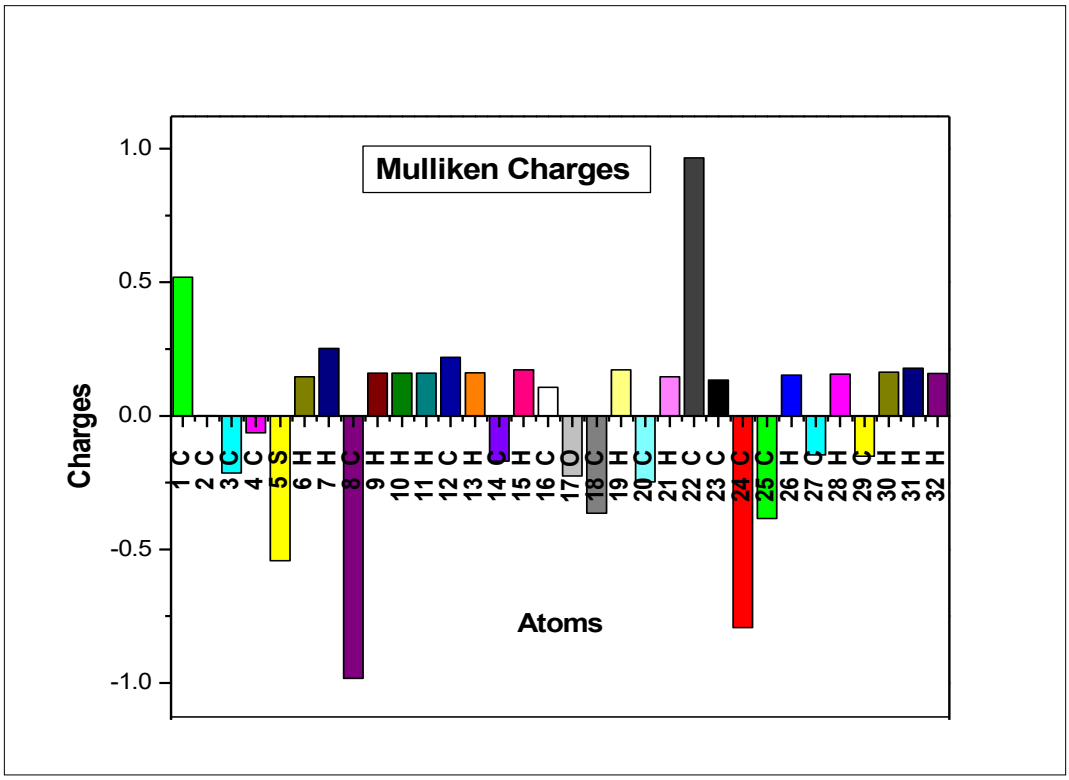

Fig. 7. Mulliken atomic charges plot of MPPO

entropy, heat capacity, enthalpy changes and temperatures were fitted by quadratic formulas and the correspondingare fitting factors (R^2) for those thermodynamic properties are 0.9999, 0.9992 and 0.9994, respectively. The corresponding fitting equations are as follows and the correlation graphics are shown in Fig. 8.

$$S^0_m = 0.98075 + 0.00414T - 3.65824 \times 10^{-5} T^2 \quad (R^2 = 0.9999)$$

$$C^0_{p,m} = 6.04475 + 0.02552T + 2.25471 \times 10^{-5} T^2 \quad (R^2 = 0.9992)$$

$$\Delta H^0_m = 4.00201 + 0.169T + 1.49276 \times 10^{-5} T^2 \quad (R^2 = 0.9994)$$

The above data can be used to compute other thermodynamic energies according to the well-known relationships of thermodynamic functions and to predict the directions of chemical reactions [52]. All the thermodynamic calculations were done in gas phase and they could not be used in solution.

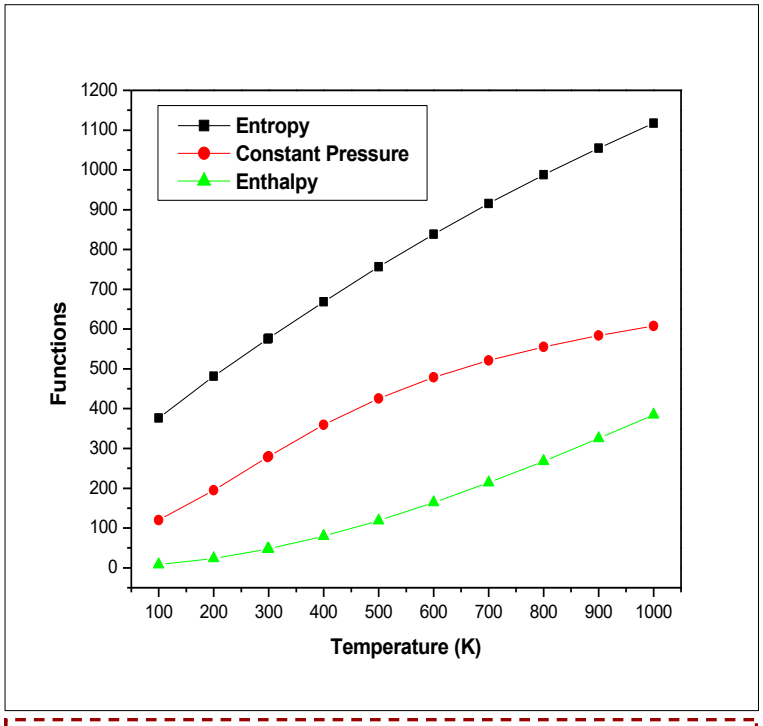

Fig. 8. The thermodynamic properties of MPPO at different

Conclusion

A complete vibrational analysis had been carried out for the first time to the molecule MPPO. The bond parameters and vibrational wavenumbers agreed well with experimental results. The first order hyperpolarizability (β_0 = 10.2328x10^{-30}esu) of MPPO was calculated and found to be twenty seven times greater than that of urea and hence the molecule had moderate NLO activity. The considerabledecrease of the lone pair orbital occupancy (1.581e) of LP(2)$S_5$was due to more $E^{(2)}$ energy transfer to anti-bonding orbital C3-C4. The Homo-Lumo energy gap was calculated about 3.4327 eV, which explain the eventual charge transfer occur within the molecule and also enhanced the biological activity. The recorded UV-Vis. spectral values agreed with calculated values. The λ_{max} (352) was assigned to π -π* type. Furthermore, the MEP and Mulliken atomic charges had been calculated and also plotted. The good correlations between the statistical thermodynamics and temperature were also established.

References:

1. Li, R., Kenyon, G.L., Cohen, F.E., Chen, X., Gong, B., Dominguez, J.N., Davison, E., Kurzban, G., Miller, R.E., Nuzman, E.O., Rosenthal, P. J., McKerrow, J.H., "In Vitro Antimalarial Activity of Chalcones and Their Derivatives", J.Med. Chem. 38 (1995) 5031-5037.
2. Ballesteros, J.F., Sanz, M.J., Ubeda, A., Miranda, M.A., Iborra, S., Paya, M., Alcaraz,M.J., "Synthesis and Pharmacological Evaluation of 2'-Hydroxychalcones and Flavones as Inhibitors of Inflammatory Mediators Generation", J. Med.Chem. 38 (1995) 2794-2797.
3. Wattenberg, L.W., Coccia, J.B., Galhaith, A.R., Galbraith, "Inhibition of carcinogen-induced pulmonary and mammary carcinogenesis by chalcone administered subsequent to carcinogen exposure", Cancer Lett. 83(1994)165-169.
4. Dinkova-Kostova, A.T., Abeygunawardana, C., Talalay, P., "Chemoprotective Properties of Phenylpropenoids, Bis(benzylidene)cycloalkanones, and Related Michael Reaction Acceptors: Correlation of Potencies as Phase 2 Enzyme Inducers and Radical Scavengers", J. Med. Chem. 41 (1998)5287–5296.
5. Satomi, Y., "Inhibitory effects of 3′-methyl-3-hydroxy-chalcone on proliferation of human malignant tumor cells and on skin carcinogenesis", Int. J. Cancer 55 (1993) 506-514.
6. Yit, C.C., Das, N.P., "Cytotoxic effect of butein on human colon adenocarcinoma cell proliferation", Cancer Lett. 82 (1994) 65–72.
7. Dimmock, J.R.,Kandepu, N.M., Hetherington, M., Quail, J.W.,Pugazhenthi, U., Sudom, A.M.,Chamankhah, M., Rose, P., Pass, E.,Alle, Halleran, S.,Szydlowski, J.,Mutus, B.,Tannous, M.,Manavathu, E.K., Myers, T.G.,Clercq, E.D.,Balzani, Js,J. Med. Chem. 41 (1998)1014–1026.
8. Mantas, A., Deretey, E., Ferretti, F.H., Estrada, M.R., Csizmadia, "Structural analysis of flavonoids with anti-HIV activity",J.Mol.Struct. 504 (2000) 171–179.
9. Sivakumar, M.,Phrabusreeneivasan, S., Kumar, V.,Doble, M.,Bioorg. Med. Chem. Lett. 17 (10) (2007) 3169.
10. Liu, X., Go, M.L., "Antiproliferative Properties of Piperidinylchalcones", Bioorg. Med. Chem. 14 (2006) 153–163.
11. Arulkumaran, R., Sundararajan, R., Vanangamudi, G., Subramanian, M., Ravi, K., Sathiyendidran, V., Srinivasan, S., Thirunarayanan, G., IUP J. Chem. 3 (1)(2010) 82-98.
12. Deng, J., Sanchez, T., Lalith, Q.A.M., "Discovery of structurally diverse HIV-1integrase inhibitors based on a chalcone pharmacophore", Bioorg. Med.Chem. 15 (14) (2007) 4985–5002.
13. Thirunarayanan, G. , J. Indian Chem. Soc. 84 (2008) 447-451.
14. Thirunarayanan, G., Surya, S., Srinivasan, S., Vanangamudi, G., Sathyendiran, V.,"Synthesis and insect antifeedant activities of some substituted styryl 3,4-dichlorophenyl ketones", Spectrochim. Acta 75A (2010) 152-156.
15. Wu, X., Wilairat, P., Go, M.L., "Antimalarial activity of ferrocenyl chalcones" Bioorg. Med. Chem. Lett. 12 (2002) 2299–2302.

16. Fouda, M.F.R., Abd-Elzaher, M.M., Abdelsamaia, R.A., Labib, A.A., "On the medicinal chemistry of ferrocene", Appl. Organometal. Chem. 21 (2007) 613–625.

17. Wu, X., Tiekink, E.R.T., Kostetski, I., Kocherginsky, N., Tan, A.L.C. Khoo, S.B.,Wilairat, P., Go, M.L., "Antiplasmodial Activity of Ferrocenyl Chalcones:Investigations into the Role of Ferrocene", Eur. J. Pharm. Sci. 27 (2006)175–187.

18. Cianci, J., Baell, J. B., Flynn, B. L., Gable W., J. A. Mould, D. Paul, Harvey, A.J., "Synthesis and biological evaluation of chalcones as inhibitors of the voltage-gated potassium channel Kv1.3", Bio. & Med. Chem.Lett. 18 (2008)2055–2061.

19. Chidankumar, C.S., Govindarasu, K., Hoong-Kun. F., Kavitha, E., Chandraju, S.,Kheng Quah, C., "Synthesis, molecular structure, spectroscopic characterization and quantum chemical calculation studies of (2E)-1-(5-chlorothiophen-2-yl)-3-(2,3,4-trimethoxyphenyl)prop-2-en-1-one", J. Mol. Struct. 1085 (2015)63–77.

20. Karunakaran, V., Balachandran, V., "Experimental and computational study on molecular structure, natural bond orbital and natural hybrid orbital analysis of non-linear optical material trans-3-(o-hydroxyphenyl-1-phenyl)-2-propen-1-one", J. Mol. Struct. 1053 (2013) 66–78.

21. Frisch et al., Gaussian 03W program, (Gaussian Inc., Walling ford CT) (2004).

22. Schlegel, H.B., "Optimization of equilibrium geometries and transition structures", J.Comput. Chem. 3 (1982) 214-218.

23. Michalska, D., Raint Program, Wroclaw University of Technology, Poland (2003).

24. Vanchinathan, K., Bhagavannarayana, G., Muthu, K., Meenakshisundaram, S.P.,"Synthesis, crystal growth and characterization of 1,5-diphenylpenta-1,4-dien-3-one: An organic crystal," Physica B 406 (2011) 4195–4199.

25. Pasterny, K., Wrzalik, R., Kupka, T., Pasterna, G., "Theoretical and experimental vibrational studies on liquid thiophene and its acetonitrile solution", J. Mol.Struct. 614 (2002) 297-304.

26. Radom, L., Scaling Fators for obtaining vibrational Frequencies and zero-point energy from HF/6-31G* and mp2/6-31G*, Harmonic Frequencies", Instrum. J.Chem.33 (1993) 345-350.

27. Socrates,G., "Infrared and Raman characteristic group frequencies-Tables and Charts", 3rd Ed., John Wiley & sons, Ltd., Chichester,2001.

28. Vein, D.L., Colthup, N.B., Fateley, W.G., Grasselli, J.G., "The Hand book of Infrared and Raman characteristic frequencies of organic molecules", Academic Press, San Diego, 1991.

29. Druz˙bicki, K., Mikuli, E., Ossowska-Chru´sciel, M.D., "Experimental (FT-IR, FT-RS) and theoretical (DFT) studies of vibrational dynamics and molecular structure of 4-n-pentylphenyl-4′-n-octyloxythiobenzoate (8OS5)", Vib. Spect. 52 (2010) 54–62.

30. Satyanarayana, D.N., "Vibrational Spectroscopy-Theory and Applications" New Delhi: New Age International (P) Ltd. Pub., 2nd Ed., 2004.

31. Balachandran,V., Janaki, A., Nataraj, A.,"Theoretical investigations on molecular structure, vibrational spectra,HOMO, LUMO, NBO analysis and hyperpolarizability calculations ofthiophene-2-

carbohydrazide", Spectrochim. Acta 118A (2014) 321–330.

32. Badawi, H. M., "Structural stability, C–N internal rotations and vibrational spectral analysis of non-planar phenylurea and phenylthiourea", Spectrochim. Acta 72 A (2009) 523-527.
33. Fleming, G. D., Koch, R, Campos Vallete, M.M., "Theoretical study of the syn and anti thiophene-2-aldehyde conformers using density functional theory and normal coordinate analysis", Spectrochim. Acta. 65 A (2006) 935-945.
34. Unal, A., Eren, B., "FT-IR, dispersive Raman, NMR, DFT and antimicrobial activity studies on 2-(Thiophen-2-yl)-1H-benzo[d]imidazole", Spectrochim. Acta 114A(2013) 129-136.
35. Tzeng, W.B., Narayanan, K., Lin, J.L., Tung, C.C., "Structures and vibrations of o-methylaniline in the S0 and S1 states studied by ab initio calculations and resonant two-photon ionization spectroscopy," Spectrochim. Acta 55A (1998) 153–162.
36. Kleinman, D.A., "Nonlinear Dielectric Polarization in Optical Media," Phy. Rev.126 (1962) 1977–1979.
37. Smith, B., "Infrared spectral Interpretation - A systematic Approach", CRC Press,New York, 1999.
38. Colthup, N.B., Daly, L.H., Wiberley, S.E., "Introduction to Infrared and Raman Spectroscopy", Academic Press, New York, 1990.
39. Sorates, G., "Infrared characteristic Group frequencies", Wiley, inter science Pub.,New York, 1990.
40. Erdogdu, Y., Gulluoğlu. M.T., "Analysis of Vibrational Spectra of 2 and 3-Methylpiperidine Based on Density Functional Theory Calculations", Spectrochim. Acta 74A(2009) 162-167.
41. Krishnakumar, V., Ramasamy, R., "Vibrational spectra and structure of 5,6-diamino uracil and 5,6-dihydro-5-methyl uracil by density functional theory calculations", Spectrochim. Acta 66A (2007) 503-511.
42. Subramanian, M.K., Anbarasan, P.M., Ilangovan, V., Babu, S.M., "FT-IR, NIRFT-Raman and Gas Phase Infrared Spectra of 3-Aminoacetophenone by Density Functional Theory and Ab Initio Hartree–Fock Calculations", Spectrochim.Acta 71A (2008)59-67.
43. Varsanyi, G., "Assignments for Vibrational Spectra of Seven Hundred Benzene Derivatives", Vol.1 and 2, Academic Kiado, Budapest, 1973.
44. Furic, K., Mohacek, V., Bonifacic, M., Štefanic, I., "Raman spectroscopic study of H2O and D2O water solutions of glycine", J. Mol. Struct. 267 (1992) 39–44.
45. Reed, A.E., Curtiss, L.A., Weinhold, F., "Intermolecular interactions from a natural bond orbital, donor-acceptor viewpoint", Chem. Rev. 88 (1988) 899–926.
46. Varsanyi, G., "Assignments of Vibrational spectra of seven Hundred Benzene derivatives", Wiley, New York, 1974.
47. Jag, M., "Organic Spectroscopy-Principle and Applications", 2nd Ed., Narosa Pub. House, New Delhi, 2001.
48. Fukui, K., Yonezawa, T., Shingu, H., "A Molecular Orbital Theory of Reactivity in Aromatic Hydrocarbons", J. Chem. Phys. 20 (1952) 722-725.